NASA Technical Paper 1045

Parametric Study of Ascent Performance of a Vertically Launched Hydrogen-Fueled Single-Stage Reusable Transport

John J. Rehder

OCTOBER 1977

NASA

NASA Technical Paper 1045

Parametric Study of Ascent Performance of a Vertically Launched Hydrogen-Fueled Single-Stage Reusable Transport

John J. Rehder

Langley Research Center
Hampton, Virginia

National Aeronautics
and Space Administration

**Scientific and Technical
Information Office**

1977

SUMMARY

The results of a parametric study of ascent performance characteristics are presented for a vertical-take-off, horizontal-landing, single-stage-to-orbit transport vehicle powered by hydrogen fuel rocket engines with a mixture of fixed- and dual-position nozzles. These data are intended to be used as a tool for rapidly providing accurate performance estimates as part of an integrated design procedure for advanced vehicles and as a guide for determining promising candidate configurations for more detailed study. The analysis has been made by systematically varying two sets of trajectory similarity parameters based on the propulsive and aerodynamic characteristics of the vehicle and by calculating a trajectory for each combination of the parameters. The propulsion parameters are the initial thrust-weight ratio, engine combination, and the two expansion ratios of the dual-position rocket nozzles. The aerodynamic parameters are the ratio of reference area to initial weight and the ratio of maximum allowable normal force to initial weight. The results from the propulsion parametric study were used in a first-order analysis to determine the effect on the performance of including the engine mass penalty. This analysis indicates that the configuration with the lowest initial mass for a given payload requires all dual-position nozzles with an initial expansion ratio of 50 and a final expansion ratio of 150.

INTRODUCTION

Historically, major aerospace programs have required long lead times between the conceptual and operational phases, with 15 years as a typical figure. It is important, therefore, to identify early in the research process technology areas which will offer significant benefits if applied to the particular concept being studied. Such an effort by the National Aeronautics and Space Administration (NASA) is currently underway with regard to space transportation systems. This effort is aimed at identifying technology areas associated with future Earth-to-orbit transportation systems which are either critical to the development of such systems or which offer a significant cost or performance advantage as a result of their development.

The approach taken by NASA has been to choose a particular space transportation concept, a single-stage-to-orbit (SSTO) vehicle, and use preliminary system design studies to determine the effects of applying various technology advancements. The SSTO concept has generated considerable interest in recent years because of its potential for substantially reducing the operational costs of placing payloads in Earth orbit and because technology has reached a point where such vehicles appear to be feasible. (See refs. 1 to 4.)

Recent studies directed by the NASA Langley Research Center, both in-house and contractual (refs. 5 and 6), have focused on an SSTO vehicle powered by hydrogen-fueled rocket engines with a combination of single-position and

advanced dual-position bell nozzles. All nozzles are at a low expansion ratio position at lift-off and the dual-position nozzles are extended to a high expansion ratio at altitude. A vehicle with this altitude-compensating device has been shown to have weight advantages over one with only single-position nozzles (ref. 5). In studying a concept, an essential element of the preliminary design process is the determination of the ascent performance of the particular vehicle being studied.

The ascent performance is generally determined by using a trajectory optimization computer program. In the case of the SSTO studies, to assess the relative merits of the many possible combinations of nozzle positions and to compare with the single-position configurations, a large number of trajectories must be calculated. However, since trajectory optimization programs are relatively large and complex, the time and cost associated with their use prohibits them from being regularly included in the design process, particularly in an automated design system like optimal design integration system (ODIN). (See ref. 7.) Therefore, a need has arisen for a rapid method for determining the ascent performance of SSTO vehicles.

The approach taken in this study has been to construct a data base of trajectory calculation results. Only vertical take-off, horizontal-landing (VTOHL) hydrogen-fueled vehicles with advanced two-position rocket nozzles were considered. The first step of the analysis was to choose a set of vehicle similarity parameters so that different size vehicles of the same shape could be compared. These parameters, including both the propulsive and aerodynamic characteristics of the vehicle, were then varied systematically over the ranges of interest and used in a trajectory optimization program to generate an inclusive matrix of trajectory results which make up the data base. The data generated by this parametric study can be used within the design process to determine an optimal vehicle design or, when analyzed independently, the data can serve as a guide for the choice of candidate vehicles for detailed study. An example of how the data can be used in a first-order sizing analysis is also included in this report.

SYMBOLS

For the parameters, E, I_{sp}, R_S, $R_{F,z}$, and $(T/W)_1$, the term g appears in the ratio definition in order to nondimensionalize the mixture of force and mass units that occurs when the International System of Units (SI) is used.

A^* engine nozzle throat area, m^2

A_e engine exit area, m^2

E engine mass coefficient, ratio of propulsion system weight over thrust, $m_e g/T$

$F_{z,max}$ maximum allowable normal force, N

g acceleration of gravity at sea level, 9.80665 m/s^2

I_{sp}	engine specific impulse, $T/\dot{m}g$, s
$\dot{m}$	engine propellant mass flow rate, kg/s
m_o	initial vehicle mass, kg
m_e	engine system mass, kg
m_f	burnout mass, kg
p_c	engine chamber pressure, Pa
p_{SL}	sea-level atmospheric pressure, 101.325 kPa
R_e	engine combination parameter, ratio of number of dual-position engines to total number of engines
$R_{F,z}$	ratio of maximum normal force to initial weight, $F_{z,max}/m_o g$
R_m	ascent mass ratio, m_o/m_f
R_m'	ascent mass ratio modified by engine mass, $m_o/(m_f - m_e)$
R_{OF}	ratio of oxidizer mass to fuel mass
R_s	ratio of reference area to initial weight, $S_{ref}/m_o g$, m^2/MN
S_{ref}	aerodynamic reference area, m^2
T	engine thrust, N
$(T/W)_1$	initial thrust-weight ratio, $T_{SL}/m_o g$
ϵ	engine nozzle expansion ratio, A_e/A^*

Subscripts:

SL	sea-level conditions
VAC	vacuum conditions
1	pertaining to conditions at lift-off
2	pertaining to conditions at nozzle transition

Abbreviations:

LH_2	liquid hydrogen
LOX	liquid oxygen
ODIN	optimal design integration system

POST	program to optimize simulated trajectories
SSME	space shuttle main engine
SSTO	single stage to orbit
U	unconstrained
VTOHL	vertical take-off, horizontal landing

METHOD OF ANALYSIS

Vehicle Description

The vehicle in this study is a hydrogen-fueled VTOHL-SSTO transport vehicle powered by a combination of rockets with single-position and dual-position bell nozzles. This configuration, shown in figure 1, was derived during in-house studies at the Langley Research Center using the optimal design integration (ODIN) program (ref. 7). These studies assumed that the vehicle meets mission requirements similar to those of the shuttle and that in two basic technology areas, structures and propulsion, 15-year advancements beyond the shuttle level have been made. In particular, a 25-percent mass reduction from a shuttle reference was used in the areas of the body, wing, tail, tanks, and landing gear. The engine characteristics are based on space shuttle main engine (SSME) technology, which incorporates a high chamber pressure and LOX/LH_2 propellants burned at a mixture ratio of 6:1, but extended to include dual-position bell nozzles. The aerodynamic coefficients of the vehicle are assumed to be those of an early shuttle orbiter design (ref. 8), chosen because this design provided a complete and consistent set of coefficients for a vehicle of the same general class as the present vehicle.

Trajectory Determination

The trajectories were calculated with the program to optimize simulated trajectories (designated POST) (ref. 9) by assuming a due east launch from Kennedy Space Center. POST is a discrete parameter targeting and optimization program having the capability to target and optimize point mass trajectories while satisfying a general user-selected set of equality and inequality constraints. In the present case, the ascent propellant requirement was minimized, subject to in-flight inequality constraints and orbital insertion conditions. Continuous engine throttling was used to limit the total vehicle acceleration to 3g. Dynamic pressure never exceeded 48 kPa during any trajectory. The total normal force was limited by an upper bound, the value of which was used as a variable in the parametric study. The altitude, velocity, and flight-path angle at trajectory termination were constrained to correspond to the perigee of a 93 × 185 km orbit.

All the trajectories were divided into seven segments. The first segment was a 7-second vertical rise followed by the second segment during which the vehicle pitched over at a constant rate for 13 seconds. Within each of the

remaining five segments, the vehicle was steered by a piecewise linear variation of angle of attack referenced to the inertial velocity vector of the vehicle. At lift-off, the entire mixture of fixed- and dual-position engines was firing in parallel, at the same expansion ratio, the dual-position nozzles being retracted to the lower expansion ratio position. At some point in the trajectory, the fixed-position engines were shut down and the dual-position nozzles were extended to the high expansion ratio. The trajectory was calculated iteratively by POST by using the initial pitch rate, the values of the attitude angles at the end of each of the last five segments, and the point of nozzle transition until the constraint values were within input tolerances and an optimality convergence criterion was satisfied. A typical trajectory is illustrated in figure 2.

Trajectory Similarity Parameters

Trajectory similarity parameters were chosen as variables for the parametric study which would allow the results of the study to be applied to similar concepts of varying size. Since trajectories are calculated by integrating acceleration with time, vehicles with similar acceleration profiles will have similar trajectories. The acceleration comes from three sources: gravity, the propulsion system, and the vehicle aerodynamic forces. All vehicles experience the same acceleration due to gravity; thus, no similarity parameter is required in this area. Since the acceleration of a body is equal to the ratio of the force on the body to the mass, quantities which affect the force-mass ratio can be used in the areas of propulsion and aerodynamics as similarity parameters.

To achieve similarity in propulsion, the equivalent thrust-mass ratio profile must be initialized at lift-off and maintained throughout the trajectory. The initial thrust-mass ratio, therefore, was chosen as a similarity parameter. In this study this ratio is nondimensionalized by the acceleration of gravity at sea level g and referred to as initial thrust-weight ratio. To match this ratio during the trajectory, the net thrust is controlled by the total vacuum thrust provided by each type of engine and the exit areas of the engines whereas the mass of the vehicle is controlled by the propellant mass flow rates. The similarity parameters used to insure the matching of these quantities are the expansion ratios (which mainly affect the mass flow rates) and the engine combinations (defined as the number of dual-position engines divided by the total number of engines).

For aerodynamic similarity, the ratio of aerodynamic force to mass must match. Since mass history is controlled by the propulsion parameters, only the aerodynamic force need be considered. Vehicles of identical shape and of any size within the range of interest will have approximately the same aerodynamic coefficients; therefore, the force produced during similar trajectories, where the angle-of-attack histories are the same, is proportional to the aerodynamic reference area. Thus, the ratio of reference area to initial mass is used as a similarity parameter. Again, the acceleration of gravity is used to normalize this quantity. The maximum normal force allowed during the trajectory directly affects the aerodynamic force history and, when nondimensionalized by dividing by the product of initial mass and acceleration of gravity, is used as a similarity parameter.

These similarity parameters, initial thrust-weight ratio $(T/W)_1$, the two expansion ratios ε_1 and ε_2, engine combination R_e, ratio of reference area to initial weight R_S, and ratio of maximum normal force to initial weight $R_{F,Z}$ were checked by calculating three trajectories with widely different values for initial mass (1 220 000, 1 700 000, and 2 240 000 kg) but with identical values for the similarity parameters. The trajectories were virtually identical within the accuracy of the trajectory optimization program.

Parametric Study Matrix

Since it was expected that the effects on the performance of varying the propulsion parameters would be independent of the effects caused by the aerodynamic parameters, two separate parametric studies were performed. Each of the propulsion parameters were varied for a fixed set of aerodynamic parameters; then the aerodynamic parameters were varied for several different combinations of propulsion parameters to demonstrate the independence.

All the trajectories calculated while varying the propulsion similarity parameters assumed the same values for initial mass, reference area, and maximum normal force. These values were 1 704 600 kg, 926.4 m^2, and 5.066 MN and are the results of an in-house point design vehicle systems study. Each of the propulsion similarity parameters took on three values as follows: expansion ratio at lift-off ε_1, 20, 50, and 80; ε_2, 100, 150, and 200; initial thrust-weight ratio $(T/W)_1$, 1.15, 1.30, and 1.45; and engine combination R_e, 0.4, 0.6, and 0.8. Also, a set of trajectories using $R_e = 0.0$, that is, all single-position nozzles, for each of the values of $(T/W)_1$ and ε_1 was calculated as a comparison with the other trajectories and to serve as a natural boundary for the parametric study. Thus, a total of $3^4 + 3^2$ or 90 trajectories were calculated for this part of the study.

Each engine was assumed to have 3 024 790 N of sea-level thrust T_{SL}. The total number of engines required for each of the desired values of $(T/W)_1$ was calculated and input into POST which allows fractional engines. The number was reduced at nozzle transition by multiplying by the desired value of R_e. Since each type of engine has the same sea-level thrust, the parameter R_e can be thought of as a thrust split. That is, R_e is equal to the sea-level thrust of the dual-position engines divided by the total sea-level thrust. The vacuum specific impulse for each expansion ratio was determined from the curve in figure 3, which was developed for use in both in-house and contractual systems vehicle studies (ref. 6). The vacuum thrust for each fixed and retracted nozzle was calculated by using the formula

$$T_{VAC} = \frac{T_{SL}}{1 - p_{SL}\left[\varepsilon/(I_{sp})_{VAC}\right](A^*/\dot{m}g)} \tag{1}$$

where p_{SL} is the sea-level atmospheric pressure, 101 325 N/m^2 and $A^*/\dot{m}g$ is a constant, 10.77 m^2-sec/MN. The mass flow rate did not change when the nozzles were extended. Thus, the vacuum thrust for the extended nozzle can be calculated by $T_{VAC,2} = T_{VAC,1}\left[(I_{sp})_{VAC,2}/(I_{sp})_{VAC,1}\right]$. The nozzle exit area

was calculated by using

$$A_e = T_{VAC}\left[\varepsilon/(I_{sp})_{VAC}\right](A^*/\dot{m}g) \tag{2}$$

Each of the aerodynamic similarity parameters took on three values by using values of 600 m^2, 926.4 m^2, and 1200 m^2 for aerodynamic reference area and values of 3.750 MN, 5.066 MN, and an unconstrained case for maximum normal force for a total of 3^2 or 9 trajectories. One trajectory, using 926.4 m^2 for reference area and 5.066 MN for maximum normal force was previously calculated in the propulsion parametric study; thus, eight calculations for each combination of propulsion parameters remained. Five such combinations were selected; as a result, there were 40 trajectories for the aerodynamic parametric study. The five combinations consisted of one case using the midpoint values of the propulsion parameters and four others each corresponding to a change in one of the four propulsion parameters from the midpoint value. In all the trajectories the performance was judged by mass ratio, defined as the ratio of initial mass to burnout mass. Performance is maximized when mass ratio is minimized.

RESULTS AND DISCUSSION

The presentation of the results of the parametric study start with figure 4. In the figures, mass ratio R_m is plotted against each of the similarity parameters. Since, for the most part, each parameter takes on only three values, the fairing of the curves is open to interpretation, particularly in the cases of $(T/W)_1$ and R_e. However, the trends shown are established by the data and a different fairing should not have any gross effects in the application of the data.

Propulsion Parameters

The results of varying the propulsion similarity parameters are presented first. Figure 4 shows that the ascent performance improves significantly with increasing $(T/W)_1$, because of reduced velocity losses caused by gravity at higher $(T/W)_1$. This trend is not appreciably altered when either R_e or ε_2 is changed as shown in figures 4(b), 4(c), and 4(d). This result was expected since changing R_e or ε_2 should have little effect on the early part of the trajectory where most of the velocity loss due to gravity occurs. For higher values of ε_1, however, the slope of the curves is less steep and the curves are closer together at a high value of $(T/W)_1$; thus, the effect of changing ε_1 is less pronounced for higher values of $(T/W)_1$. This condition is due to the decrease in the trajectory time with a high $(T/W)_1$ since any change in ε_1 will have less time to take effect.

The relationship between mass ratio and engine combination is shown in figure 5. For the case where $(T/W)_1 = 1.30$, $\varepsilon_1 = 50$, and $\varepsilon_2 = 150$, trajectories were also calculated for $R_e = 0.1$, 0.2, and 0.3 to help define the curves. In general, R_m decreases as R_e increases. This effect is very pronounced at the low value of ε_1 and almost disappears at the high value, since, for high values of ε_1, there is less difference between ε_1 and ε_2.

In fact, if ε_1 and ε_2 are equal, R_e has no meaning and the trajectory is similar to the single-position nozzle case. For a given ε_1, changing ε_2 does not have a large effect on the shape of the curves except where R_e is small. This is to be expected since the curves for a particular ε_1 must converge at $R_e = 0$, where the parameter ε_2 is no longer effective. Comparing figures 5(a), 5(b), and 5(c) indicates that the shape of the curves is not affected appreciably by $(T/W)_1$, although the sets of curves for particular values of ε_1 are closer together for the higher values of $(T/W)_1$ because of, as discussed previously, the decrease in flight time.

The variation of performance with ε_1 is illustrated in figure 6. For the smaller values of $(T/W)_1$, R_e, and ε_2, the reduction of mass ratio with increasing ε_1 is significant. As noted before, at higher values of $(T/W)_1$ the effect of changing ε_1 is decreased. However, at the high values of R_e and ε_2, the performance of the extended nozzles is dominant and the effect of ε_1 is almost negligible.

Figure 7 shows that the performance improves with increasing ε_2 because of the increasing vacuum specific impulse. This result, in addition to the trends displayed by the previous figures, indicates that based strictly on trajectory analysis, the best performance can be achieved by using dual-position nozzles on all the engines with $\varepsilon_1 = 50$, $\varepsilon_2 = 200$, and $(T/W)_1 = 1.45$. However, this conclusion may not prove to be true when a more complete vehicle design is determined, since dual-position nozzles are heavier and engine weight increases with expansion ratio. Also, that particular propulsion system configuration may not be physically realizable in a realistic design. Even so, the data provides inputs to the design process and gives clues to help the designer choose promising candidates for further study.

Aerodynamic Parameters

The results of varying the aerodynamic similarity parameters are displayed in figures 8 and 9. In each of the four parts to these figures, the plots of the trajectory results using the midpoint values of the propulsion parameters ($(T/W)_1 = 1.3$, $R_e = 0.6$, $\varepsilon_1 = 50$, and $\varepsilon_2 = 150$) are repeated as solid curves so that any change in the relationships due to changes in the propulsion parameters will be visible. The plots using a different value for each propulsion parameter appear as dashed curves.

Figure 8 shows that the mass ratio increased essentially linearly with increasing R_s, the ratio of reference area to initial weight. During the portion of the trajectory where the aerodynamic forces are the greatest, the vehicle is forced to fly at a low angle of attack (less than 10°) because of the upper bound placed on normal force. Increasing R_s would cause the angle of attack to decrease even more to satisfy the normal-force constraint. Since the angle of attack is less than that for maximum lift-drag ratio (ref. 8), decreasing the angle decreases lift-drag ratio and causes more drag for approximately the same amount of lift. Therefore, the increase in mass ratio is caused by the increased velocity loss due to drag. This relationship is not affected by the maximum normal force as illustrated by the curves being nearly parallel. Comparing the dashed curves with the solid curves in figures 8(a) to 8(d) shows

that the linear dependence is preserved despite changing each of the propulsion parameters. In fact, the relationships among the positions and slopes of the dashed curves are essentially the same as among the solid curves and support the assumption made earlier that the two sets of parameters, propulsion and aerodynamic, could be considered independently.

The results of varying $R_{F,z}$, the ratio of maximum normal force to initial weight, are illustrated in figure 9. The maximum value of $R_{F,z}$ for each curve is the value obtained when the constraint on maximum normal force is removed. The mass ratio decreased monotonically with increasing $R_{F,z}$. This relationship, caused by a reduction in gravity losses due to increased lift, is more pronounced at the smaller values of $R_{F,z}$, although even there the dependence is not substantial. Changing R_s does not appreciably affect the trend, except that higher values of $R_{F,z}$, in the unconstrained case, are obtained with larger values of R_s.

In comparing figures 9(a) to 9(d), the dashed curves are, for the most part, essentially parallel to the solid curves, the only exception being in figure 9(a) where $(T/W)_1$ is varied. This difference comes from the higher rate of increase in velocity due to the larger $(T/W)_1$ which, in turn, causes the point of maximum normal force to occur earlier in the trajectory. However, this difference is slight, and the assumption that the two sets of similarity parameters can be considered independently remains intact.

First-Order Vehicle Sizing Analysis

To investigate the effect that engine mass has on overall vehicle mass and to demonstrate an application of the trajectory data base to the process of designing a vehicle, a first-order vehicle sizing analysis was performed. For this analysis, the performance was measured by a modified mass ratio defined as

$$R_m' = m_o/(m_f - m_e) \tag{3}$$

where m_e is the total engine mass. The engine mass is calculated for a given set of propulsion similarity parameters by

$$m_e = (m_o/T_{SL})(T/W)_1\left[(1 - R_e)E_1(T_{VAC,1}) + R_eE_2(T_{VAC,2})\right] \tag{4}$$

where E_1 and E_2 are the mass coefficients of the single- and dual-position engines, respectively. These coefficients are obtained from figure 10, which was derived for use in in-house advanced vehicle studies. The values of m_f are provided by the current propulsion parametric study. Some of the values were obtained by interpolating in both R_e and ϵ.

The optimum performance occurs when R_m' is a minimum. This can be thought of as the vehicle with the lowest initial mass for a given payload. The results are displayed in figures 11 and 12. For brevity, only the cases where $(T/W)_1 = 1.30$ are presented.

Figure 11 shows the variation of performance with engine combination. Comparing this variation with that of figure 5(b) indicates that the main effect of including engine mass is to degrade the performance for high values of ε_1. This reduction in performance is caused by the mass penalty of the higher expansion ratio overwhelming the slight performance gains shown in figure 5(b). This effect is seen more clearly in figure 12 where the variation of performance with ε_1 is shown. For values of R_e less than or equal to 0.7, the minimum of R_m' occurred at an ε_1 between 40 and 60, whereas for $R_e = 1.0$, R_m' increases monotonically with increasing ε_1. The minimum value of R_m' occurs when $\varepsilon_1 = 20$, $\varepsilon_2 = 200$, and $R_e = 1.0$. These trends are very different from those in figure 6(c) which underscores the importance of finding an optimal vehicle using an integrated design process rather than relying on trajectory analysis alone.

CONCLUDING REMARKS

A data base of ascent performance calculations has been developed for a vertically launched, hydrogen-fueled, single-stage-to-orbit vehicle concept. This data base was obtained by systematically varying a set of similarity parameters based on the vehicle propulsion and aerodynamic characteristics. The propulsion similarity parameters were initial thrust-weight ratio $(T/W)_1$, engine combination R_e, and the two expansion ratios of the dual-position nozzles ε_1 and ε_2. This data base is intended for use as an integral part of a design process for rapidly estimating vehicle performance.

The performance was shown to be strongly dependent on $(T/W)_1$ and ε_2 and in both cases improved as the value of the parameter increased. The effect of R_e and ε_1 on the performance is very pronounced for small values of those parameters but becomes almost negligible at the high values. In both cases, the mass ratio generally decreases as either ε_1 or R_e increases. These trends indicate that an optimum vehicle would have a high initial thrust-weight ratio and would use all dual-position nozzles with a first expansion ratio of 50 and a second expansion ratio of 200.

The aerodynamic similarity parameters, assumed to be independent of the propulsion parameters, were the ratio of reference area to initial weight R_S, and the ratio of maximum normal force to initial weight $R_{F,z}$. The performance is degraded substantially when R_S is increased because of the larger velocity losses due to drag. Varying $R_{F,z}$ had no effect on this trend. The performance improved slightly when $R_{F,z}$ increased because of smaller velocity losses due to gravity and higher lift. Changing the propulsion parameters had negligible effects on the result of the aerodynamic parametric study and established the validity of the assumption that the two sets of similarity parameters could be considered independently.

The results from the propulsion parametric study were applied to a first-order sizing analysis in which the effect of including the engine mass into the performance measurement was studied. The result was that the performance gains realized by increasing the initial expansion ratio were more than offset by the

increased engine mass. Therefore, the ε_1 for optimum performance was reduced from 50 to 20.

Langley Research Center
National Aeronautics and Space Administration
Hampton, VA 23665
September 8, 1977

REFERENCES

1. Salkeld, Robert: Mixed-Mode Propulsion for the Space Shuttle. Astronaut. & Aeronaut., vol. 9, no. 8, Aug. 1971, pp. 52-58.

2. Salkeld, Robert; and Beichel, Rudi: Reusable One-Stage-to-Orbit Shuttles: Brightening Prospects. Astronaut. & Aeronaut., vol. 11, no. 6, June 1973, pp. 48-58.

3. Salkeld, Robert: Single-Stage Shuttles for Ground Launch and Air Launch. Astronaut. & Aeronaut., vol. 12, no. 3, Mar. 1974, pp. 52-64.

4. Henry, Beverly Z.; and Decker, John P.: Future Earth Orbit Transportation Systems/Technology Implications. Astronaut. & Aeronaut., vol. 14, no. 9, Sept. 1976, pp. 18-28.

5. Eldred, Charles H.; Rehder, John J.; and Wilhite, Alan W.: Nozzle Selection for Optimized Single-Stage Shuttles. [Preprint] IAF-76-162, Oct. 1976.

6. Haefeli, Rudolph C.; Littler, Ernest G.; Hurley, John B.; and Winter, Martin G.: Technology Requirements for Advanced Earth-Orbital Transportation Systems - Final Report. NASA CR-2866, 1977.

7. Glatt, C. R.; and Hague, D. S.: ODIN: Optimal Design Integration System. NASA CR-2492, 1975.

8. Rainey, Robert W.; Ware, George M.; Powell, Richard W.; Brown, Lawrence W.; and Stone, David R.: Grumman H-33 Space Shuttle Orbiter Aerodynamic and Handling-Qualities Study. NASA TN D-6948, 1972.

9. Brauer, G. L.; Cornick, D. E.; and Stevenson, R.: Capabilities and Applications of the Program To Optimize Simulated Trajectories (POST). NASA CR-2770, 1977.

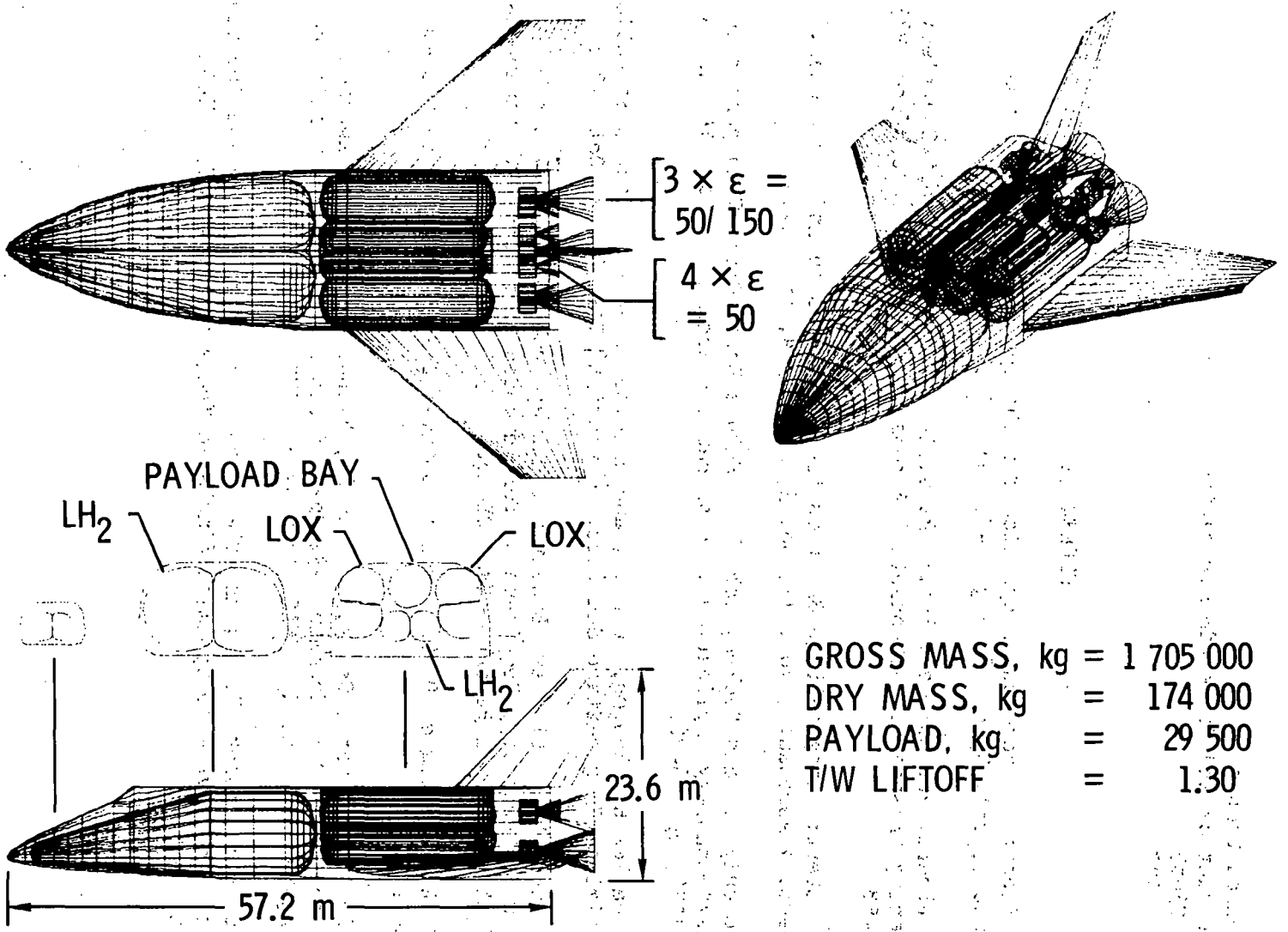

Figure 1.- Typical SSTO configuration.

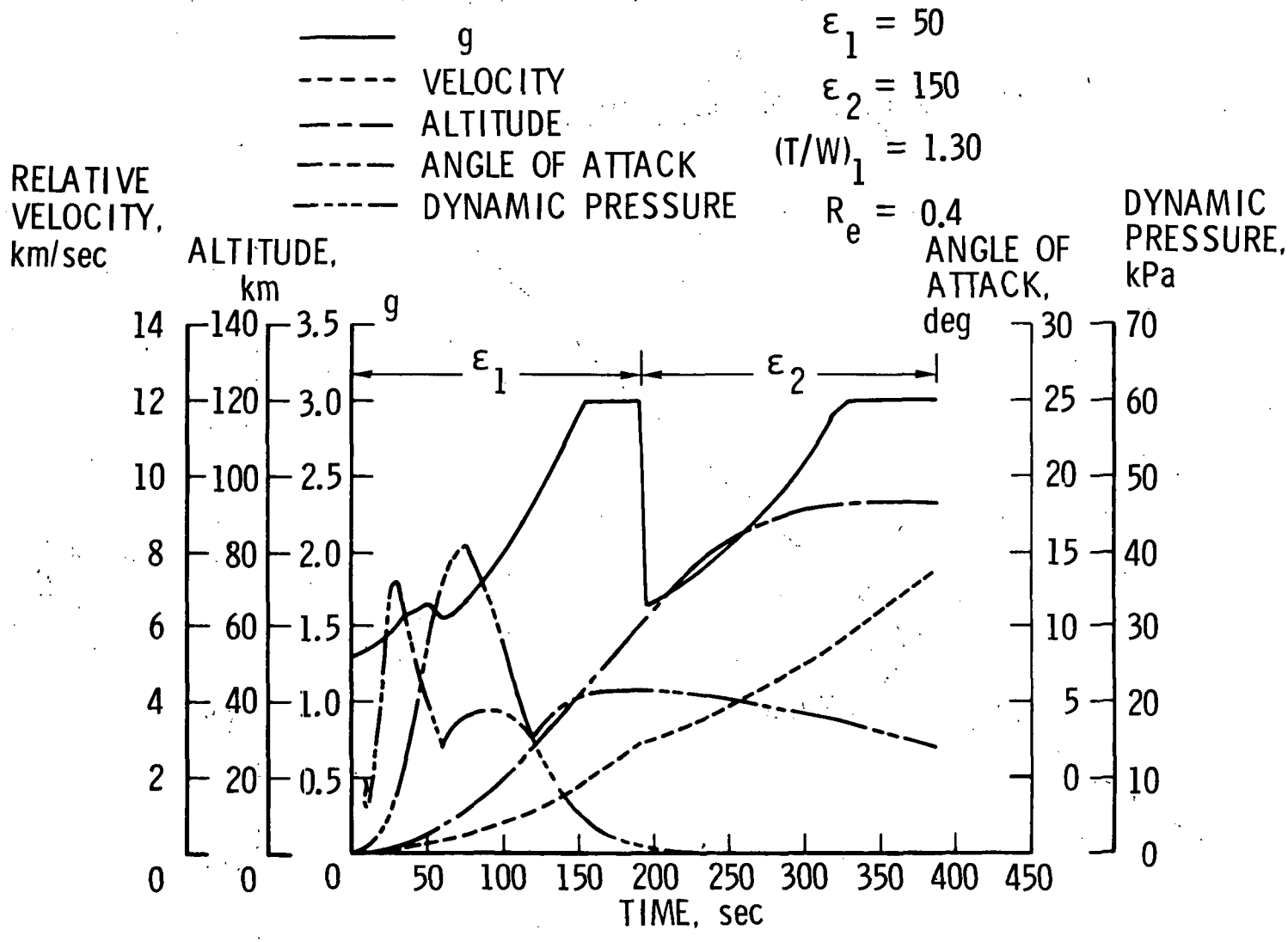

Figure 2.- Typical ascent trajectory parameters.

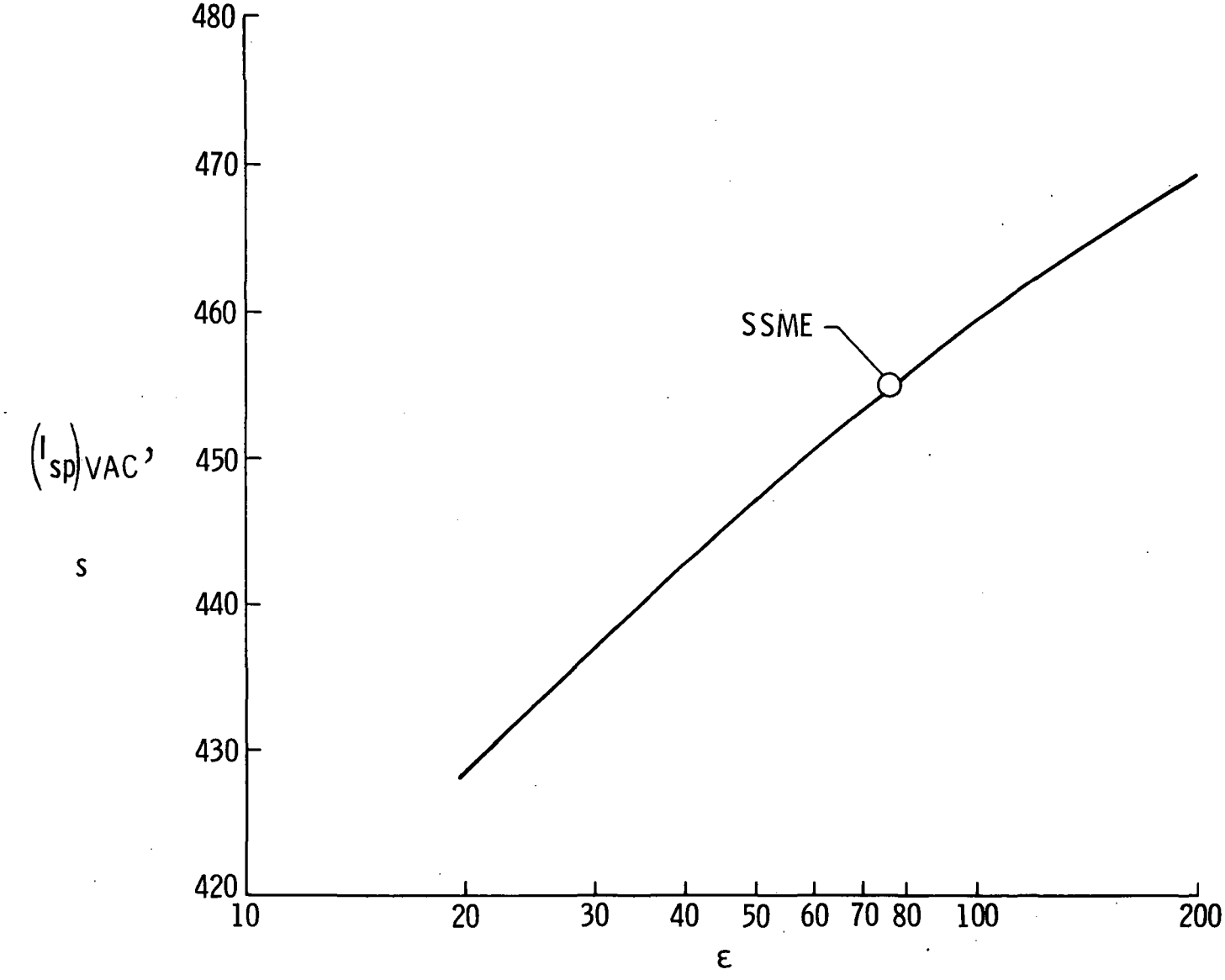

Figure 3.- Variation of vacuum specific impulse with expansion ratio. LOX/LH_2; R_{OF} = 6.0; and p_c = 20.7 MPa.

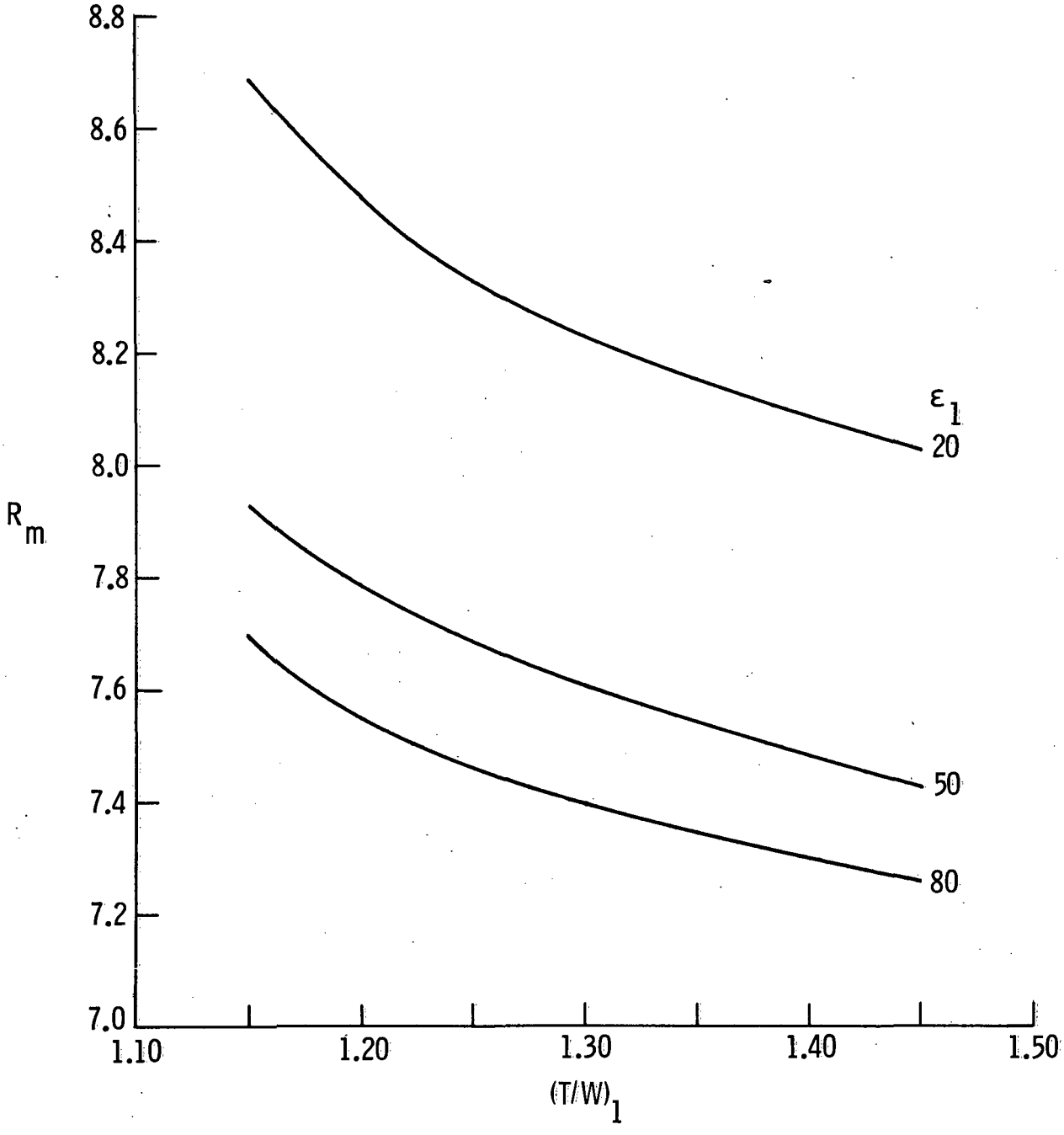

(a) $R_e = 0.0$.

Figure 4.- Variation of mass ratio with initial thrust-weight ratio.

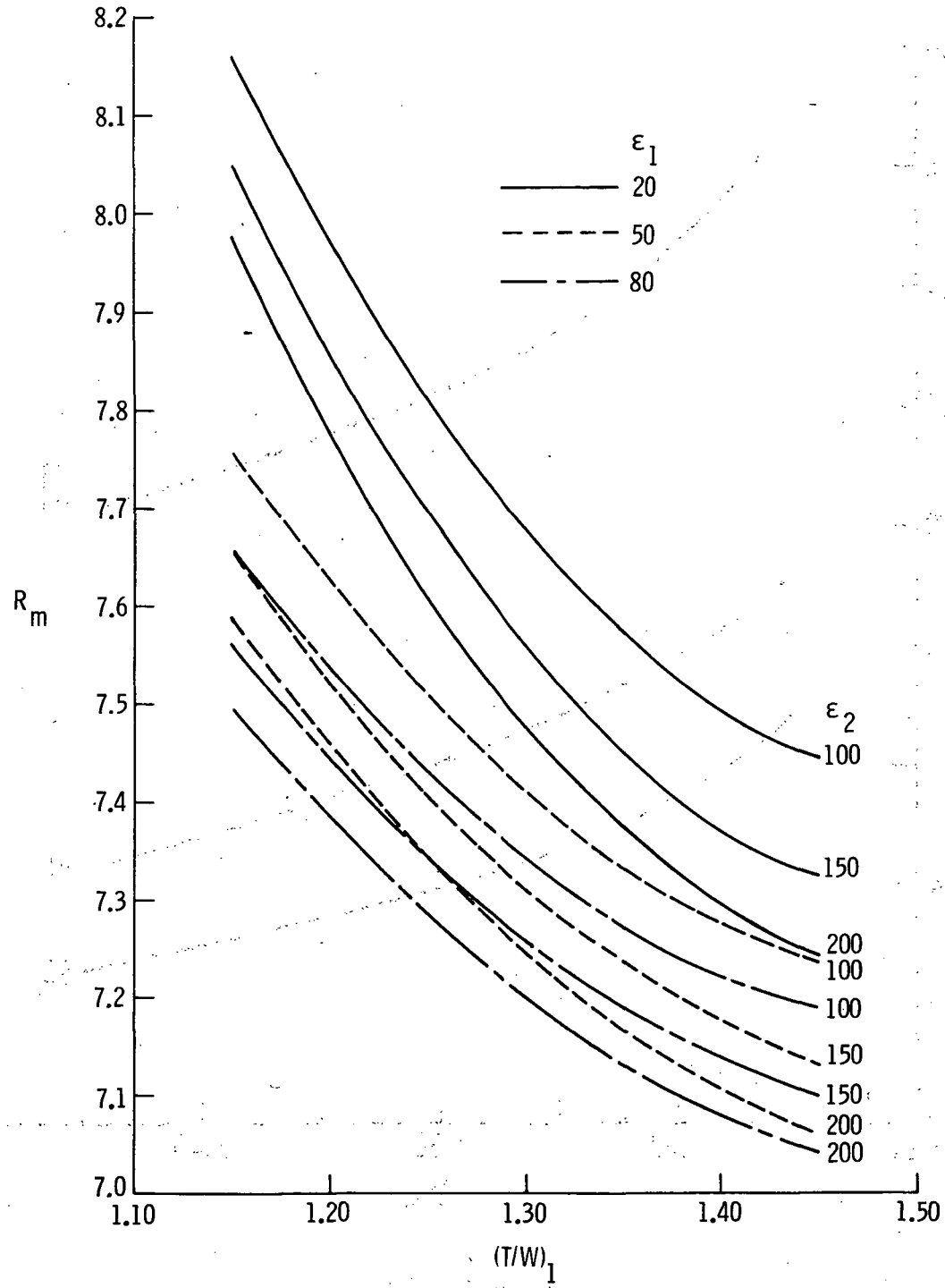

(b) $R_e = 0.4$.

Figure 4.- Continued.

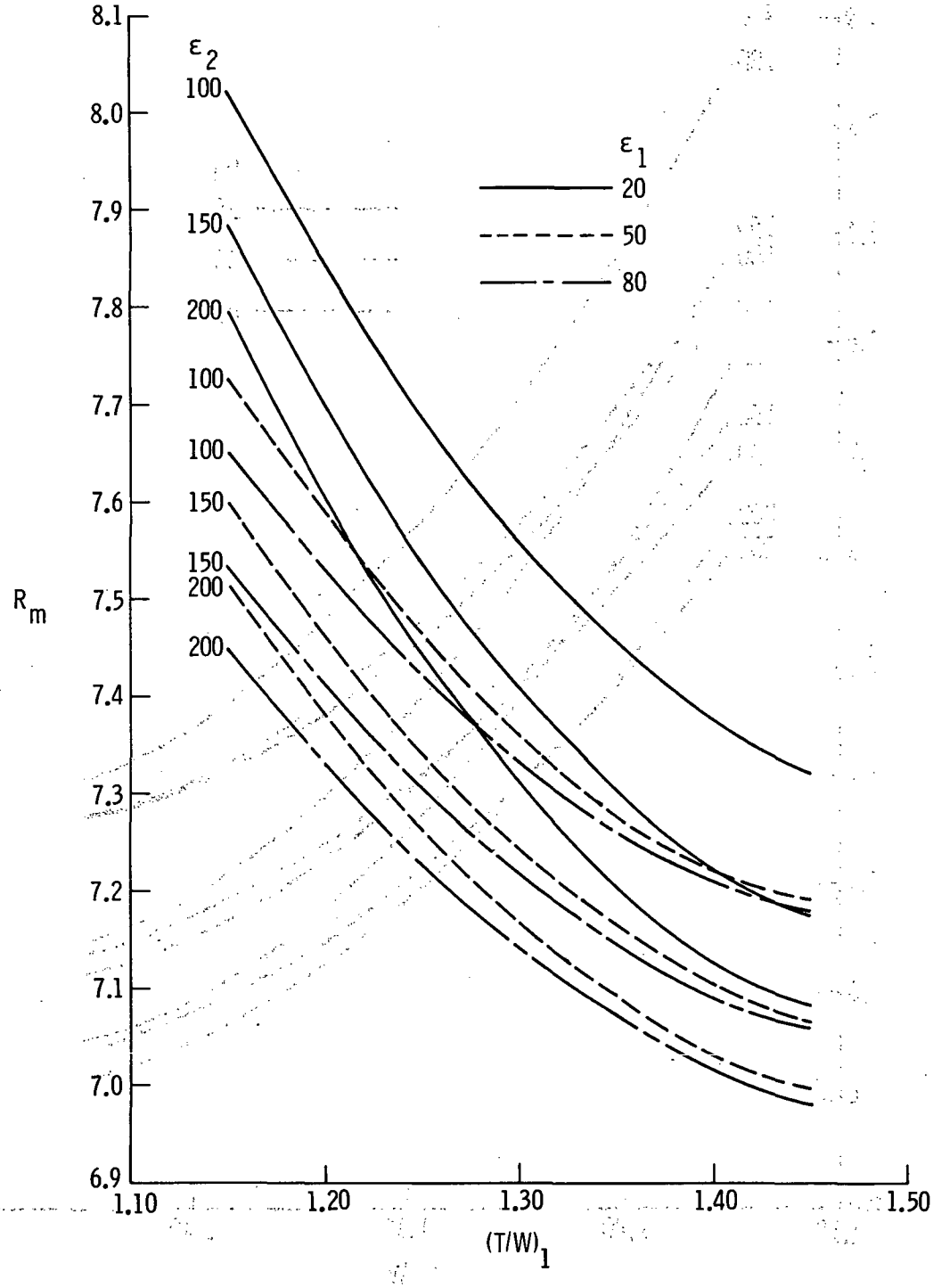

(c) $R_e = 0.6$.

Figure 4.- Continued.

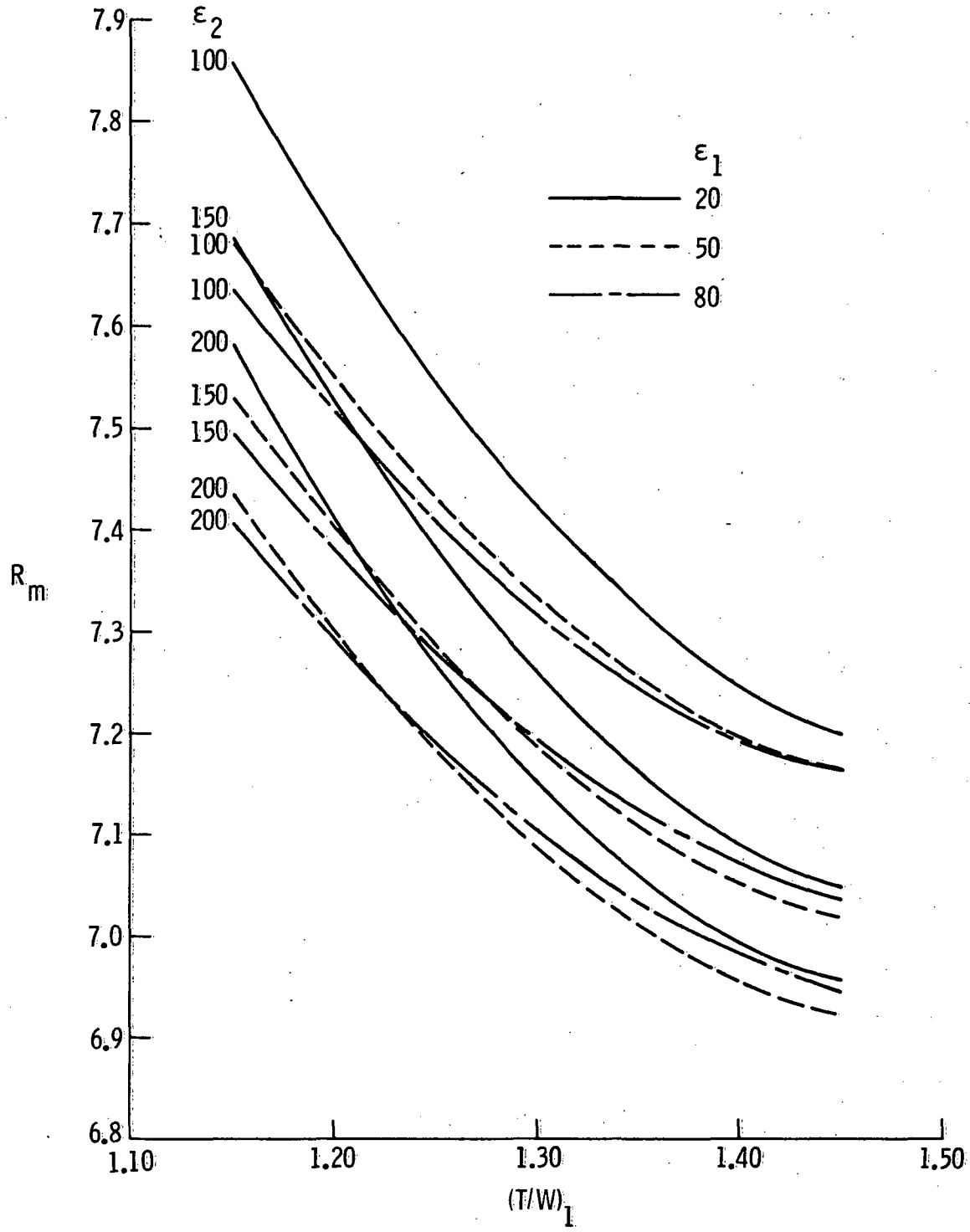

(d) R_e = 0.8.

Figure 4.- Concluded.

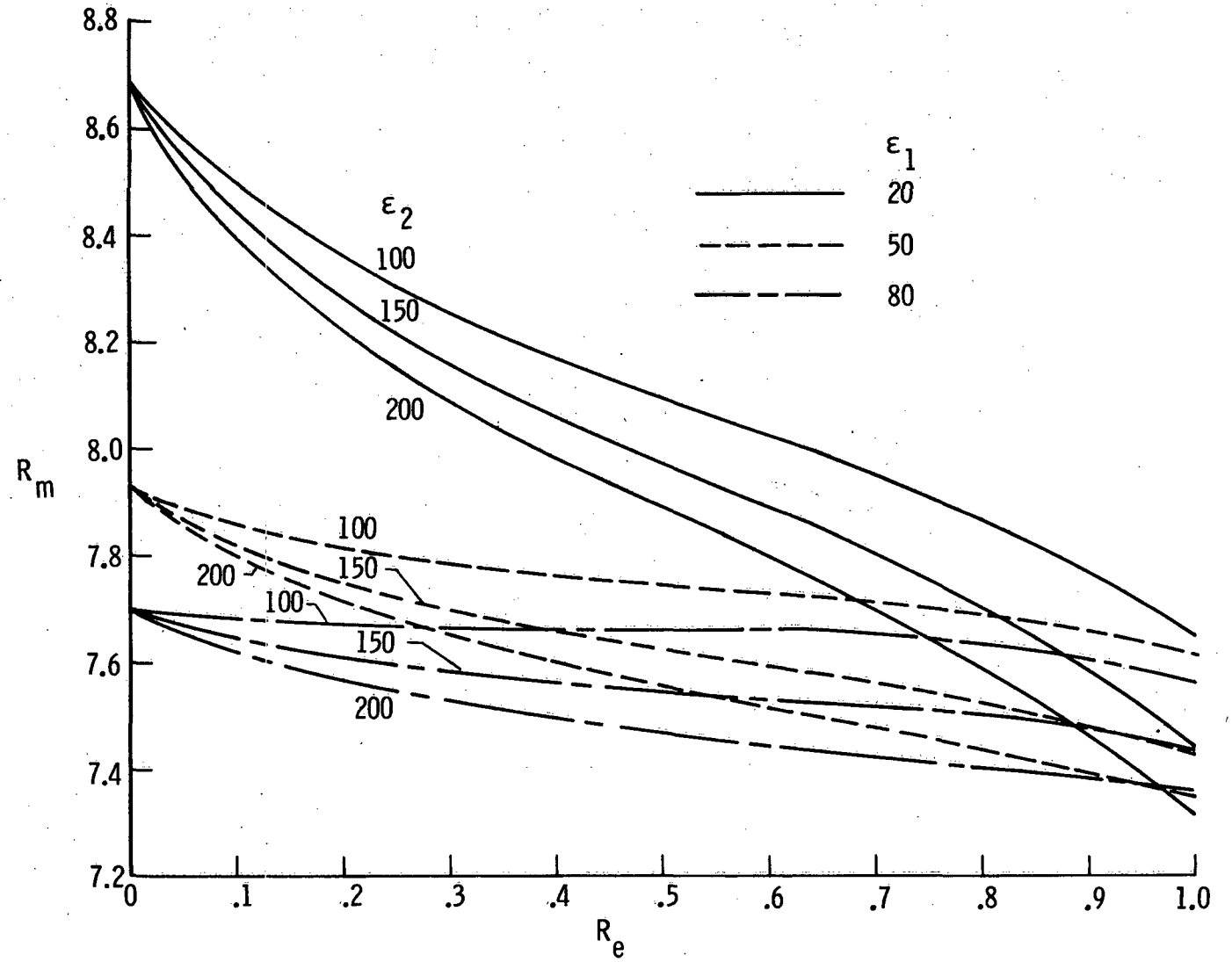

(a) $(T/W)_1 = 1.15$.

Figure 5.- Variation of mas ratio with engine combination.

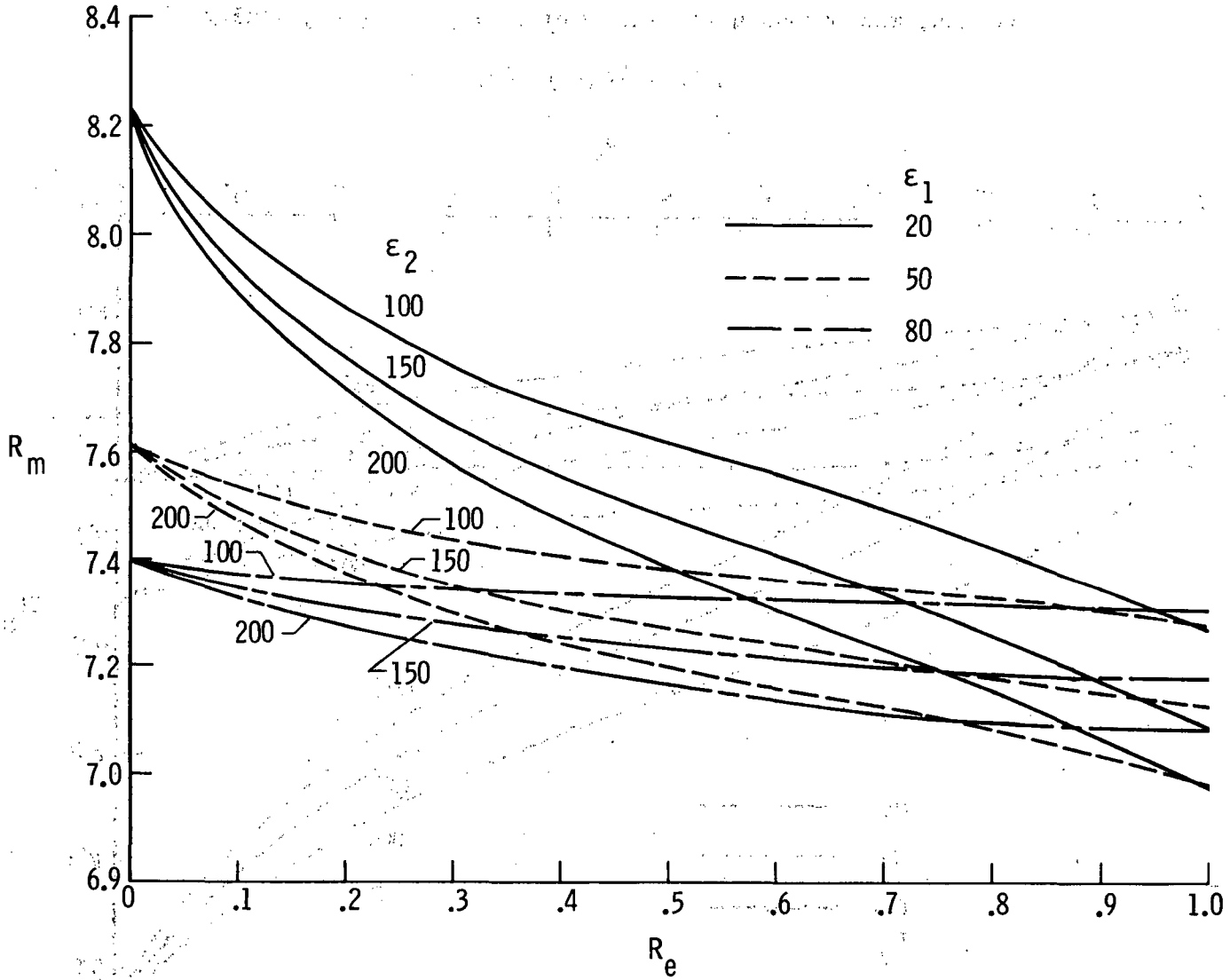

(b) $(T/W)_1 = 1.30$.

Figure 5.- Continued.

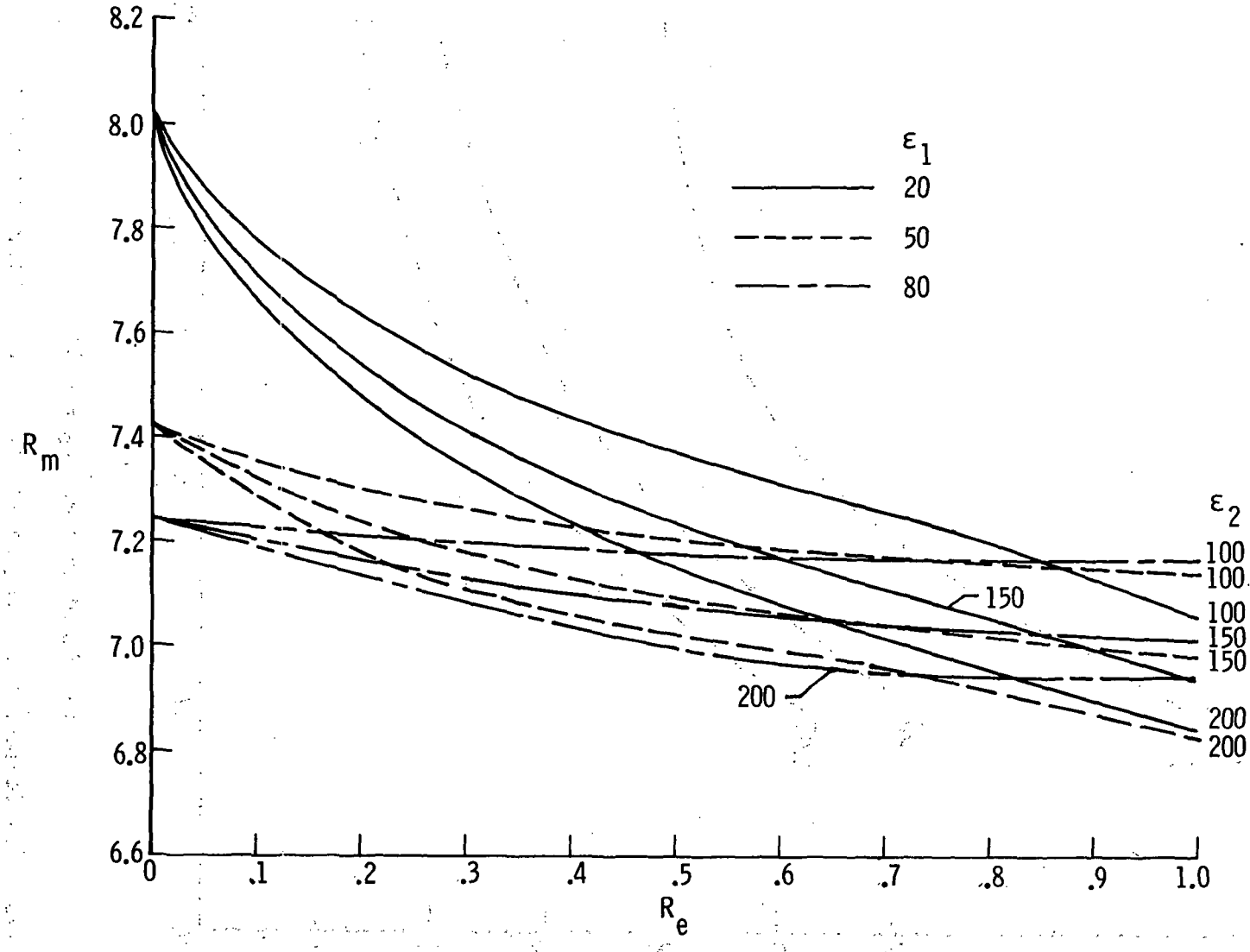

(c) $(T/W)_1 = 1.45$.

Figure 5.- Concluded.

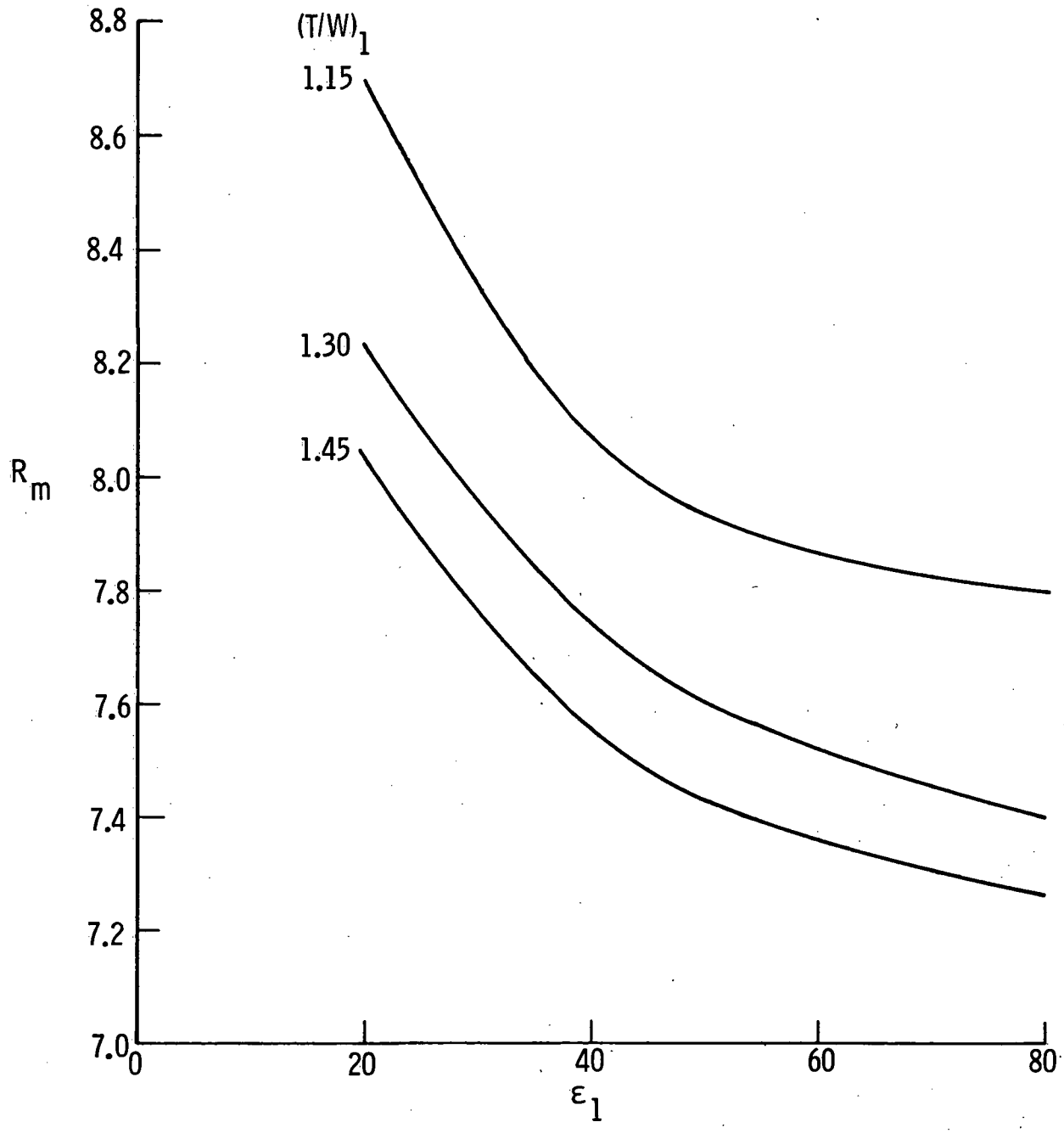

(a) Fixed nozzles (R_e = 0.0).

Figure 6.- Variation of mass ratio with initial expansion ratio.

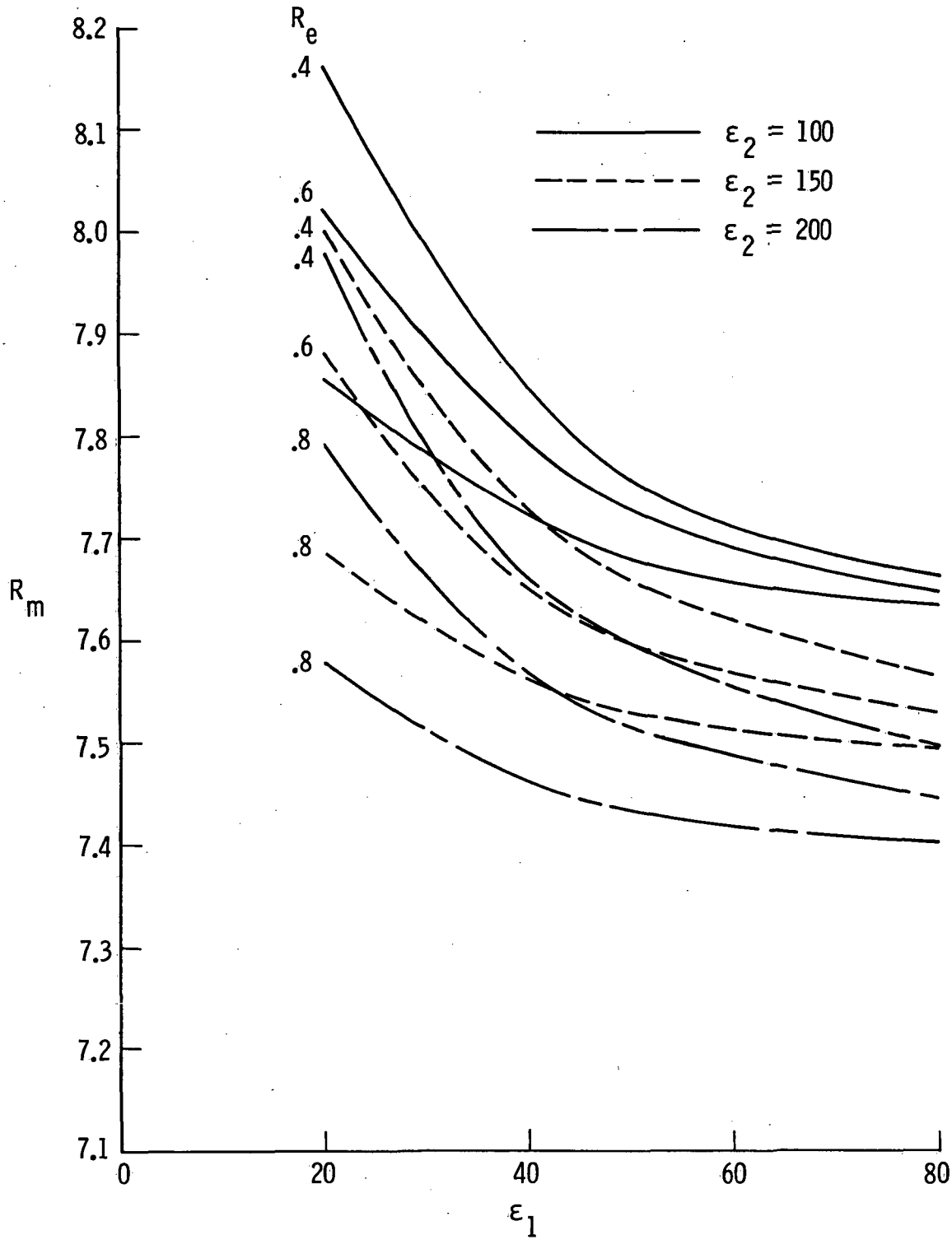

(b) Dual-position nozzles. $(T/W)_1 = 1.15$.

Figure 6.- Continued.

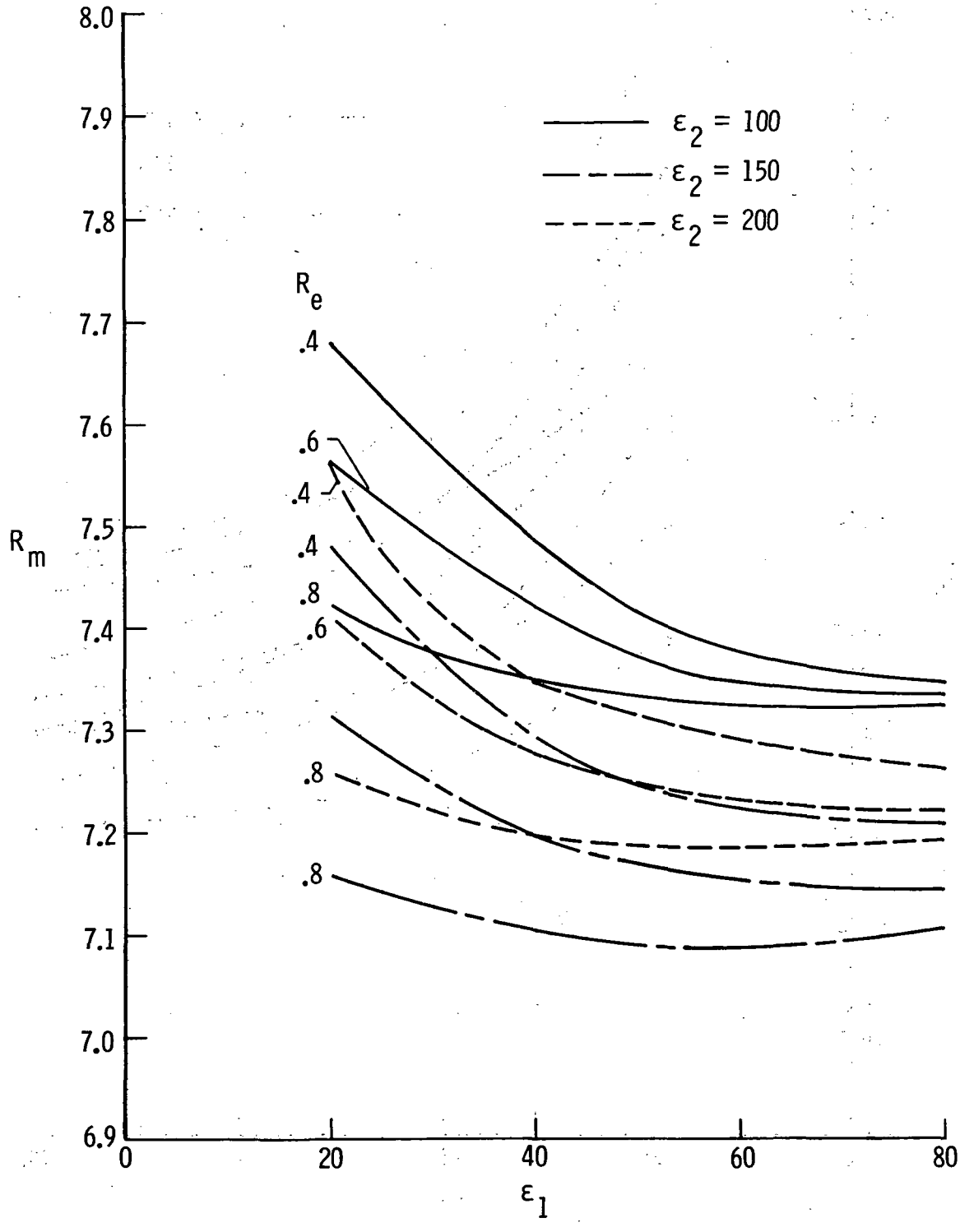

(c) Dual-position nozzles. $(T/W)_1 = 1.30$.

Figure 6.- Continued.

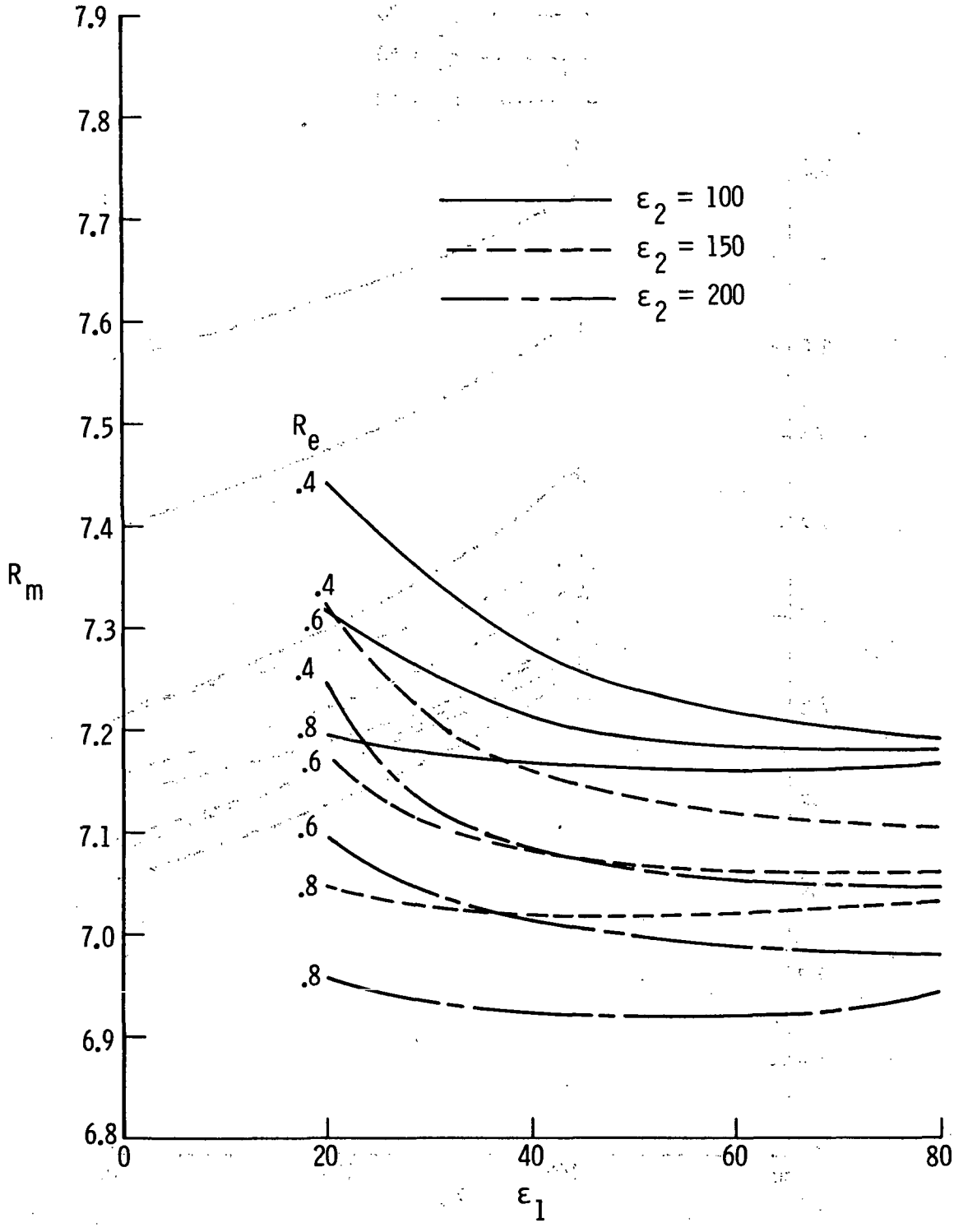

(d) Dual-position nozzles. $(T/W)_1 = 1.45$.

Figure 6.- Concluded.

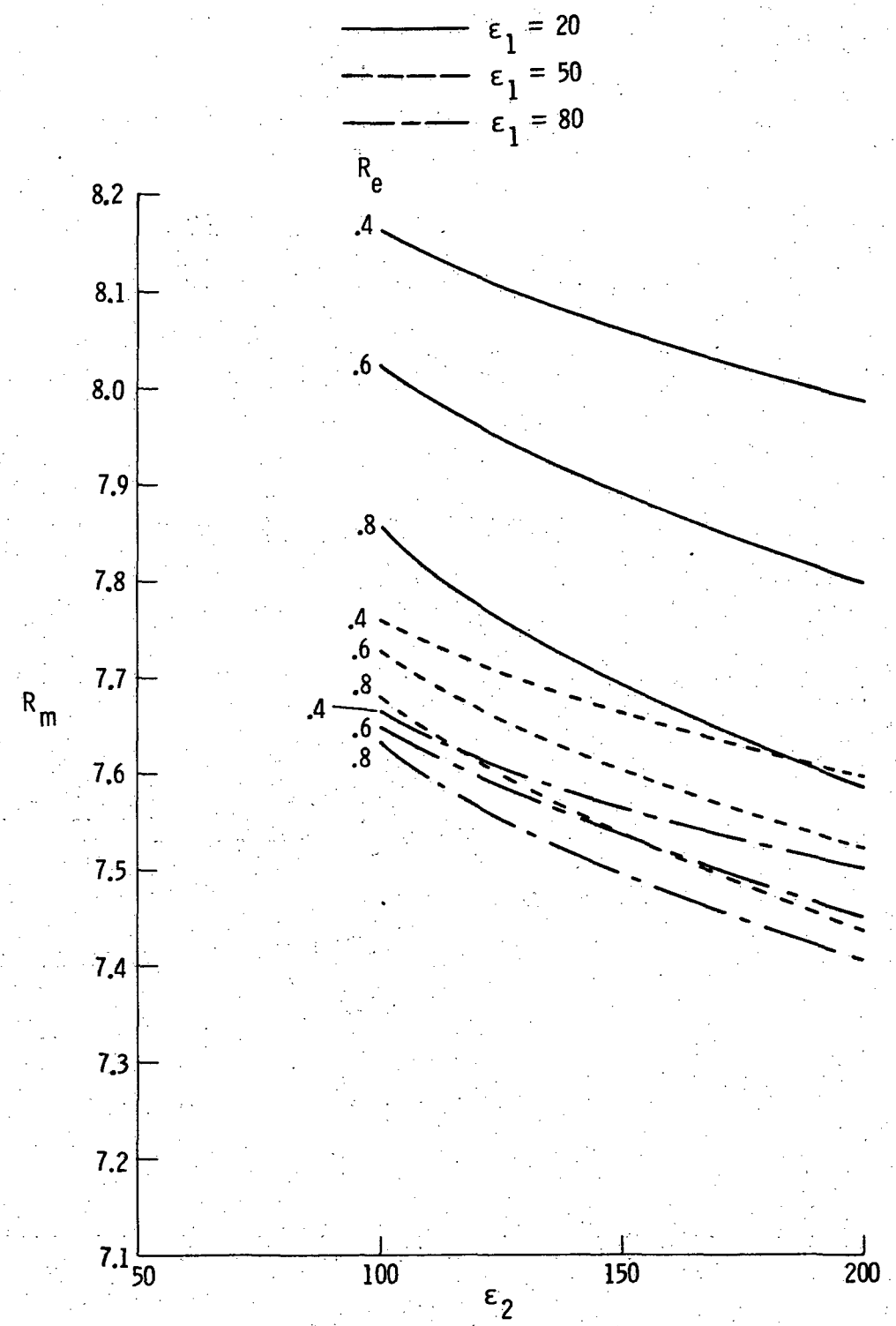

(a) $(T/W)_1 = 1.15$.

Figure 7.- Variation of mass ratio with second expansion ratio.

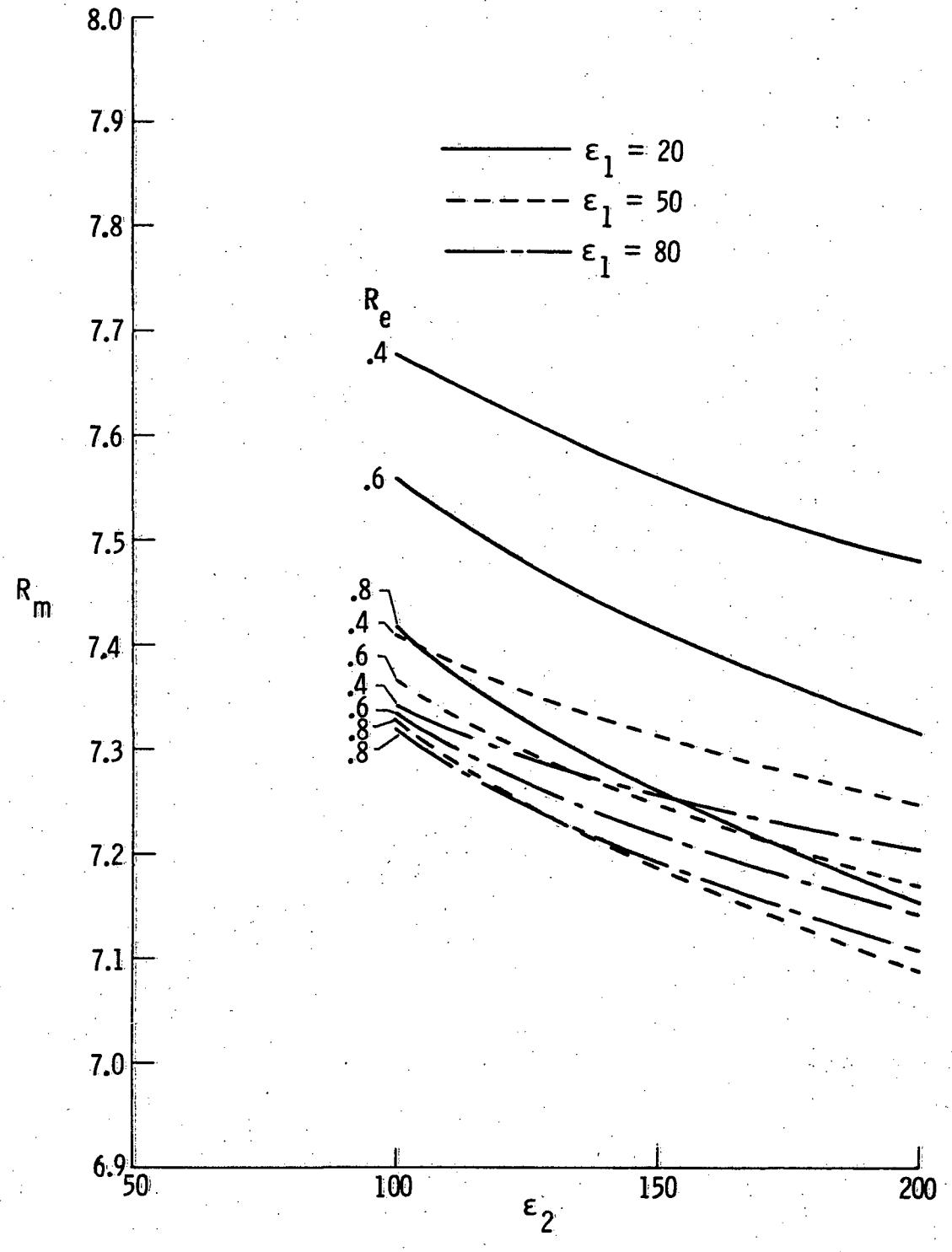

(b) $(T/W)_1 = 1.30$.

Figure 7.- Continued.

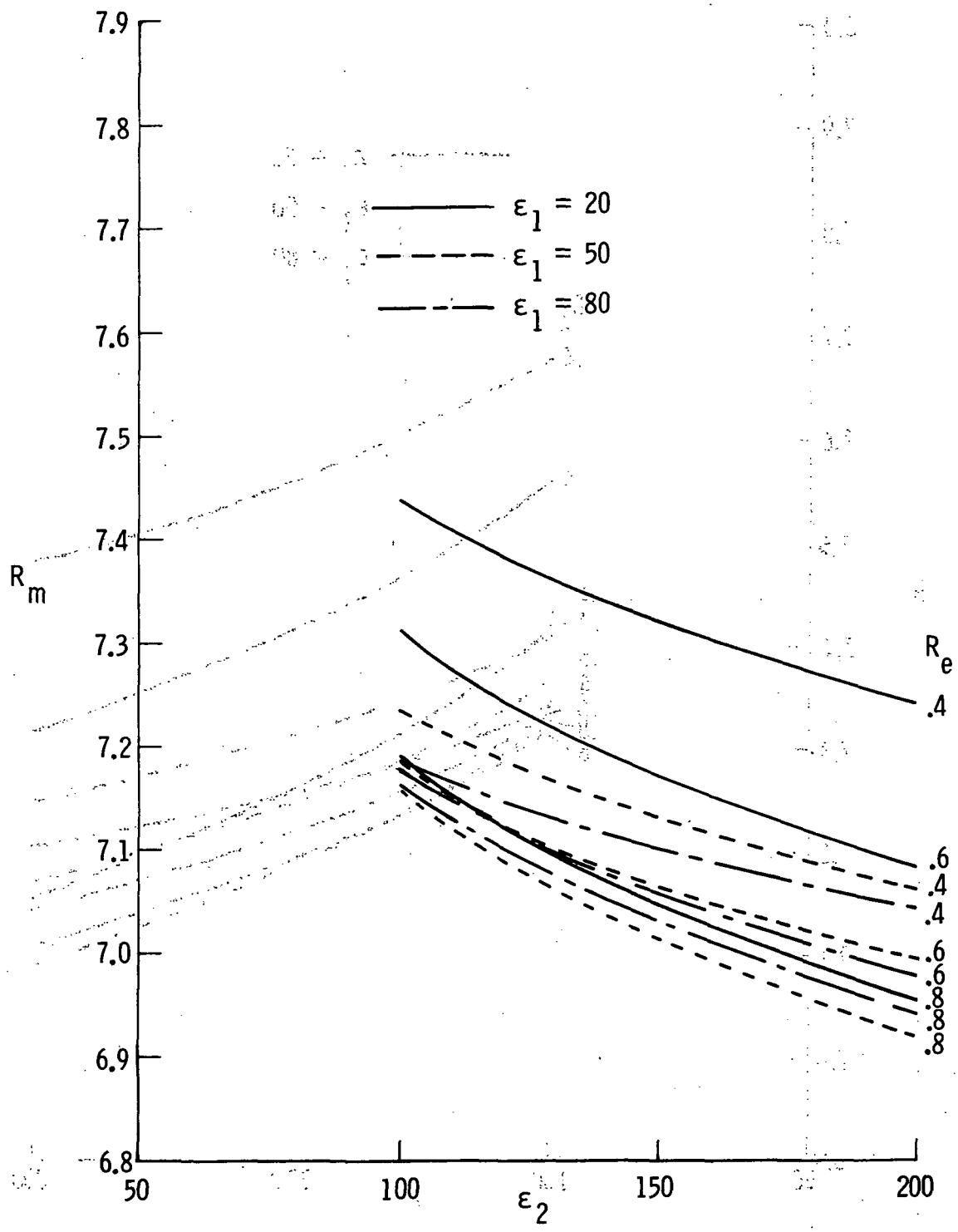

(c) $(T/W)_1 = 1.45$.

Figure 7.- Concluded.

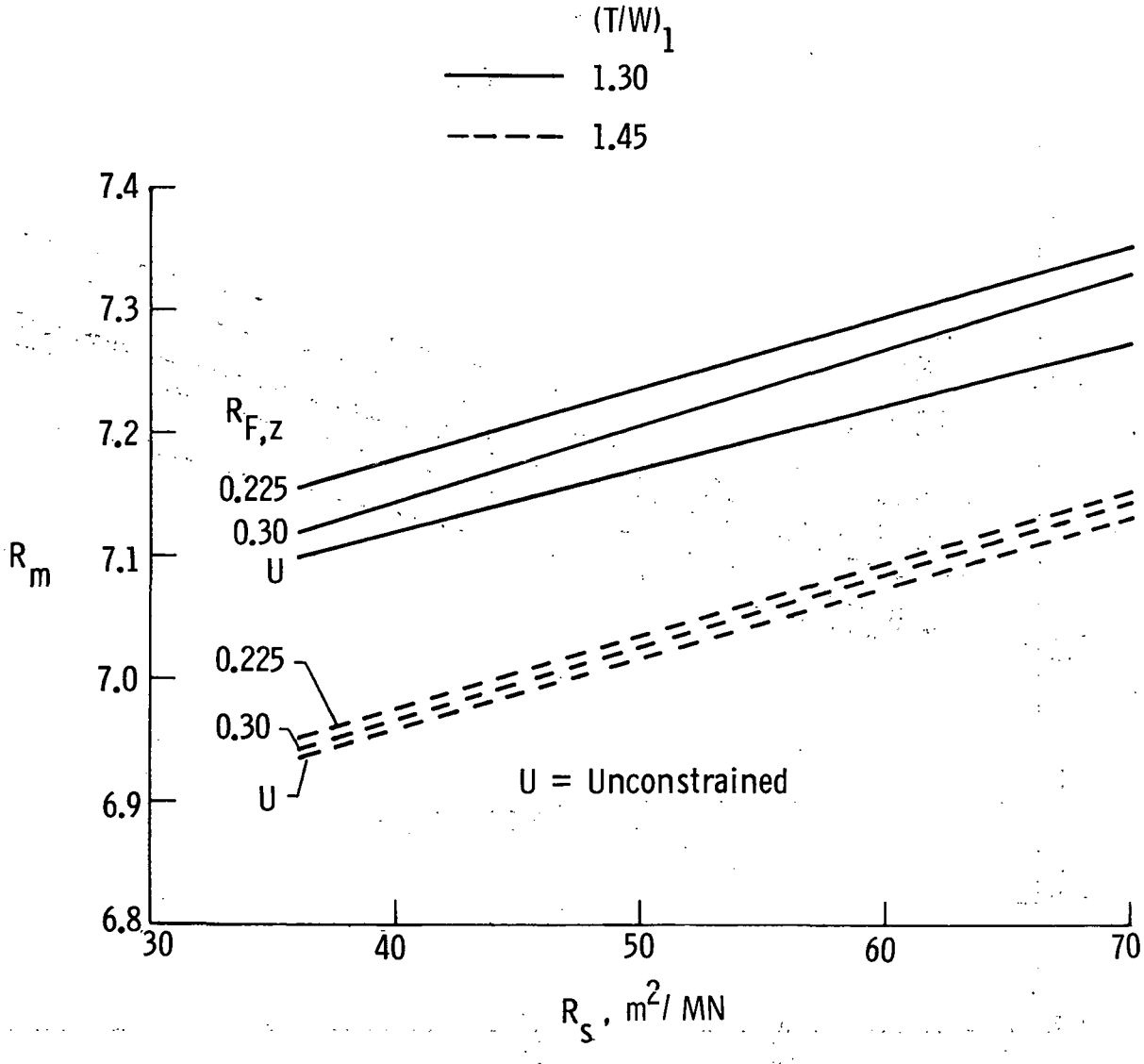

(a) Effect of $(T/W)_1$.

Figure 8.- Variation of mass ratio with ratio of reference area to initial weight.

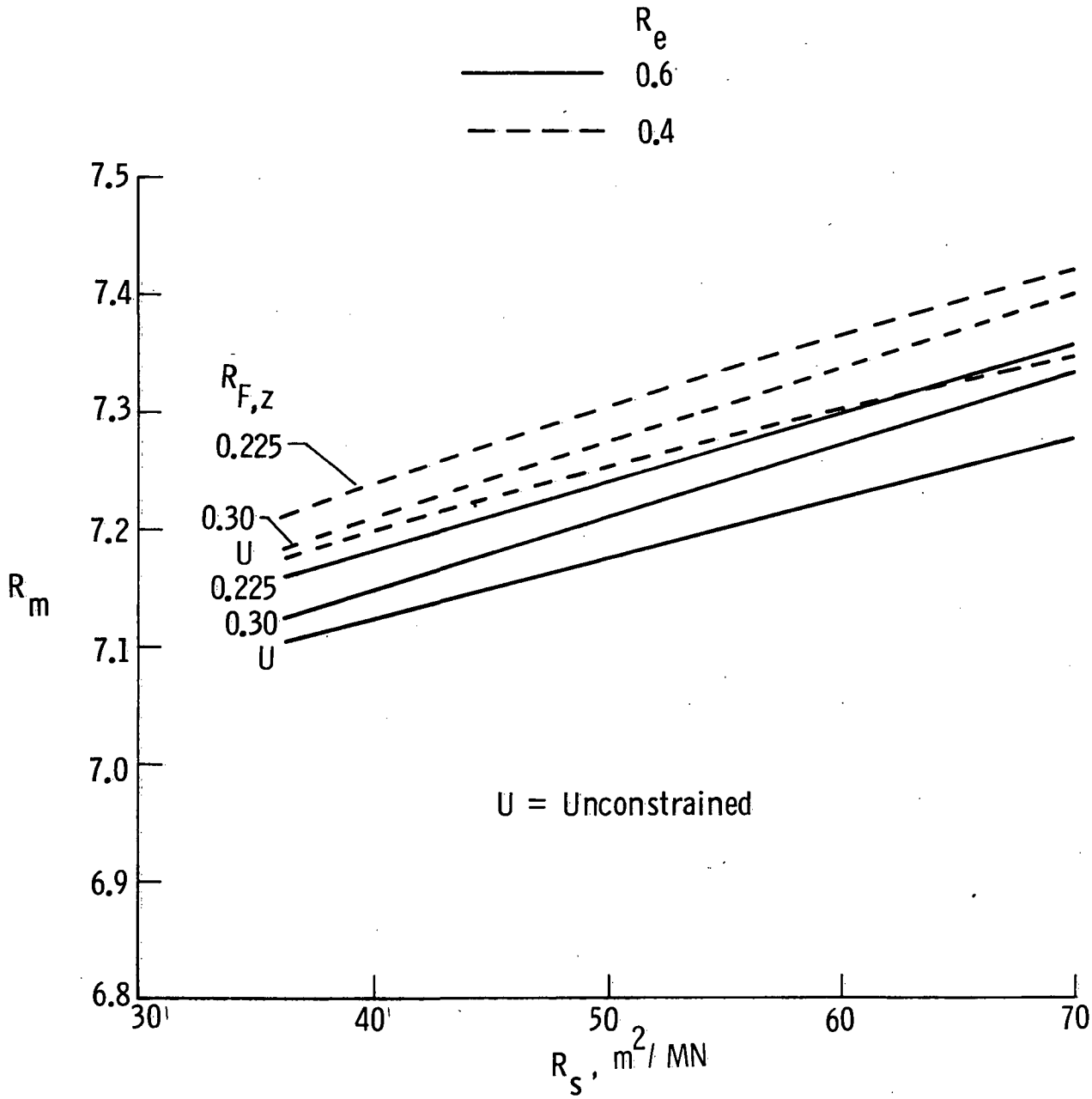

(b) Effect of R_e.

Figure 8.- Continued.

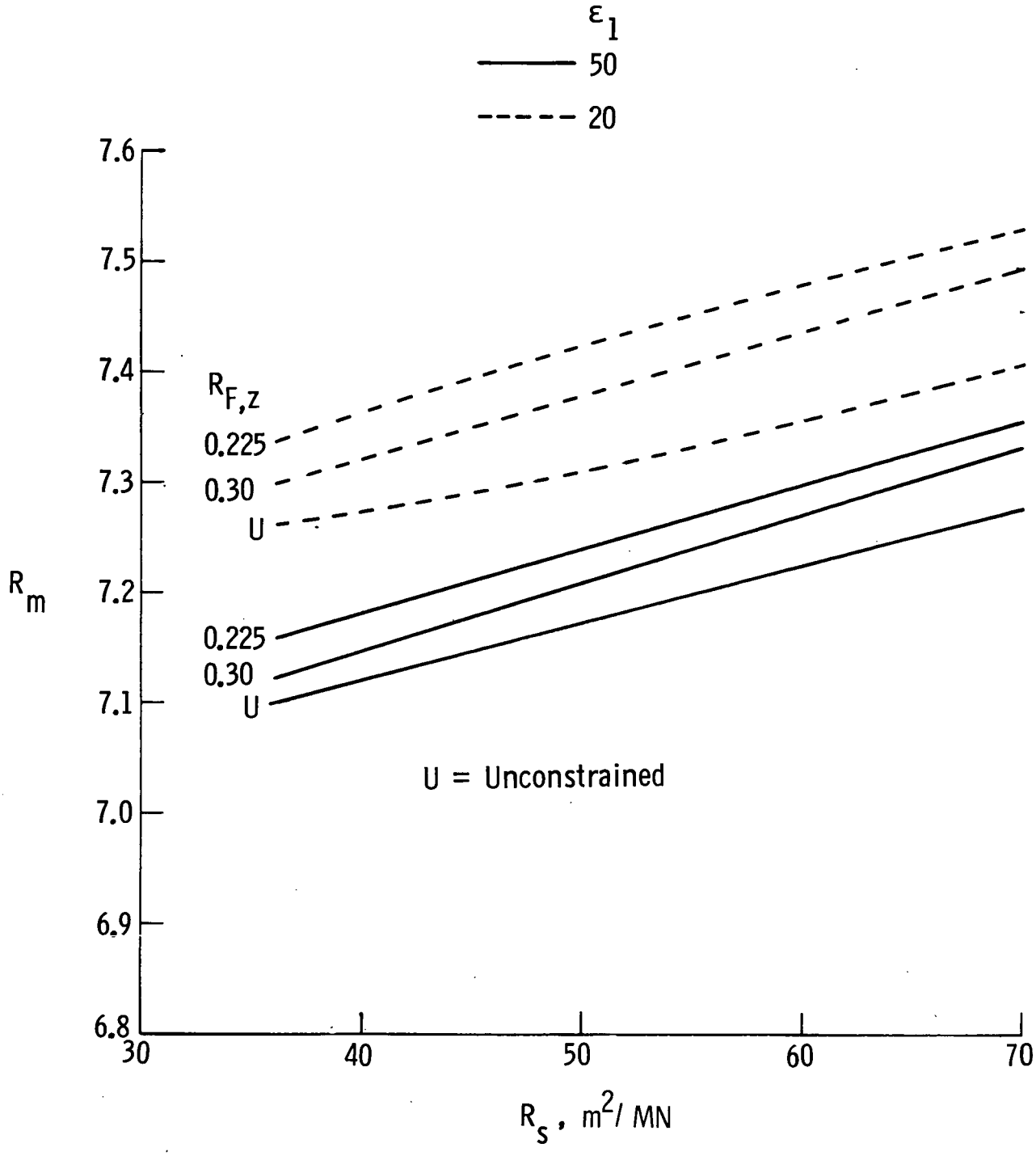

(c) Effect of ε_1.

Figure 8.- Continued.

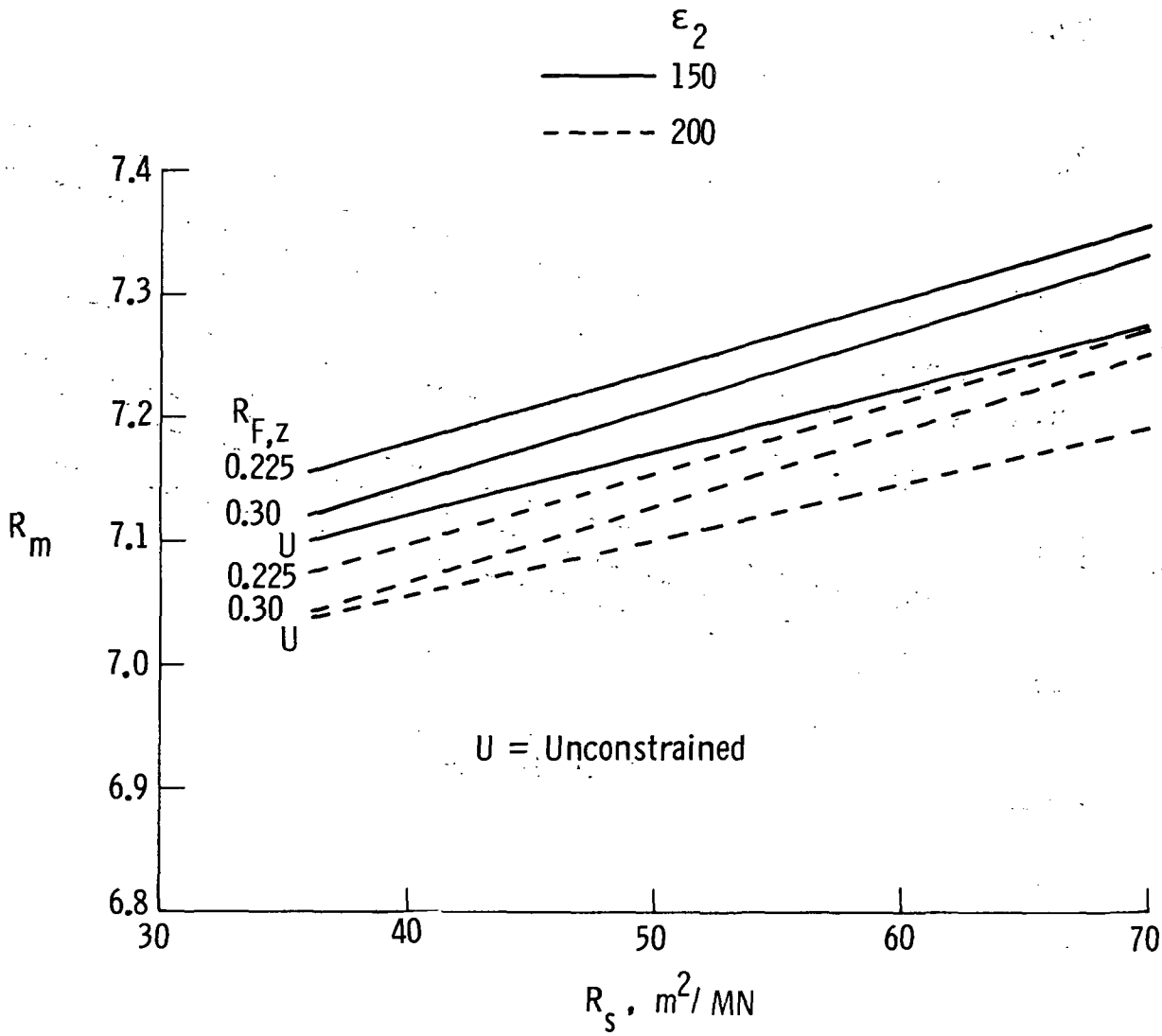

(d) Effect of ε_2.

Figure 8.- Concluded.

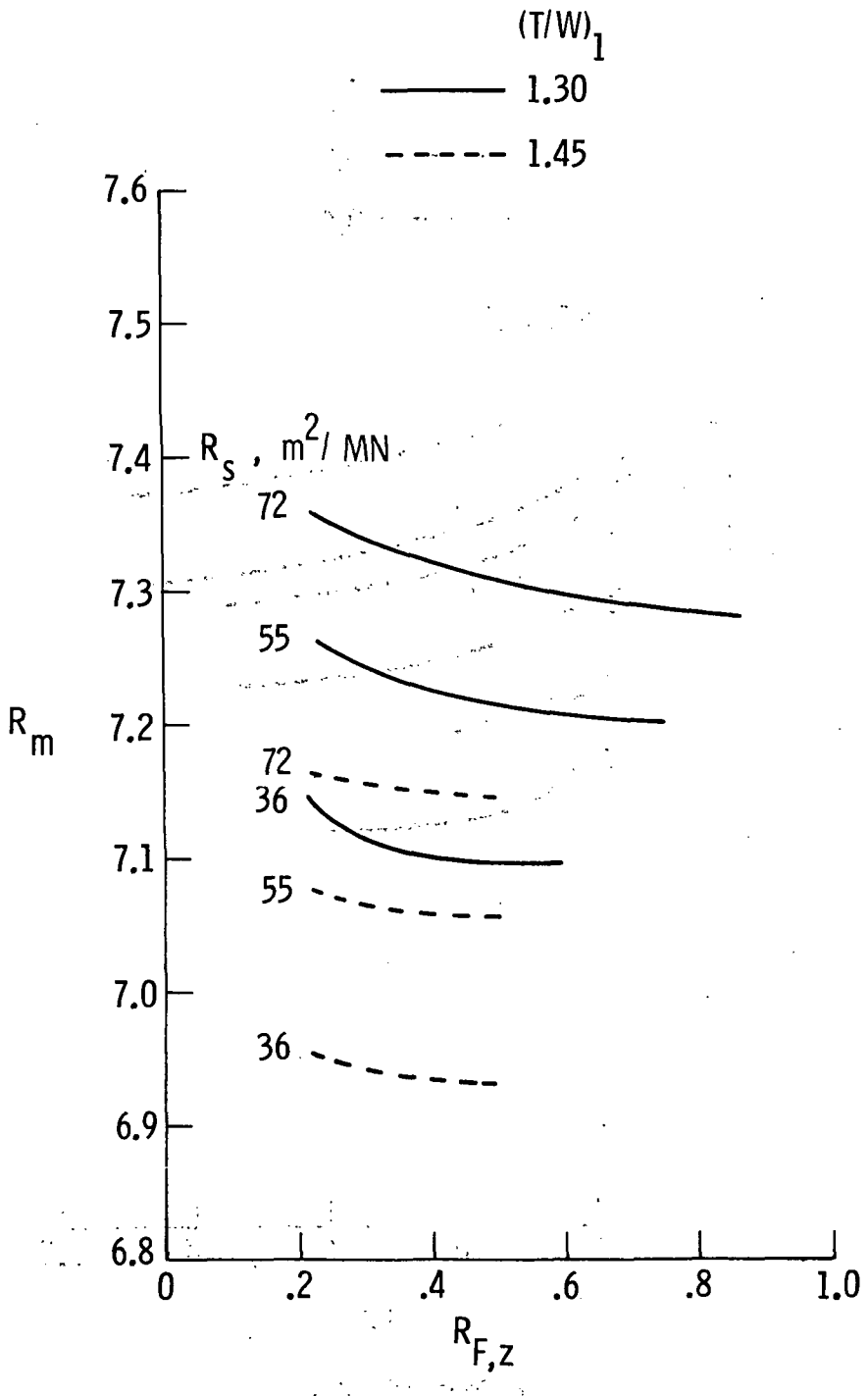

(a) Effect of $(T/W)_1$.

Figure 9.- Variation of mass ratio with ratio of maximum normal force to initial weight.

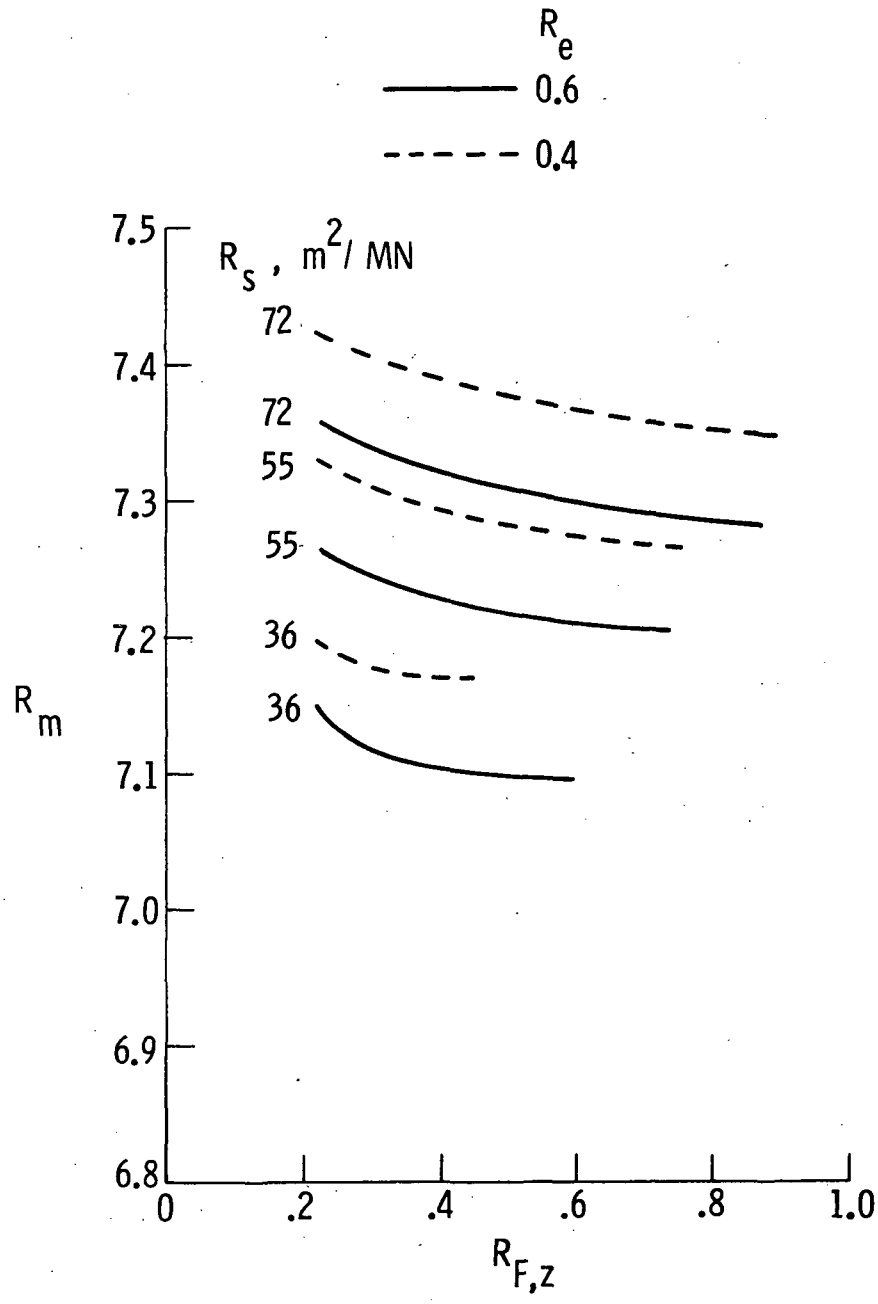

(b) Effect of R_e.

Figure 9.- Continued.

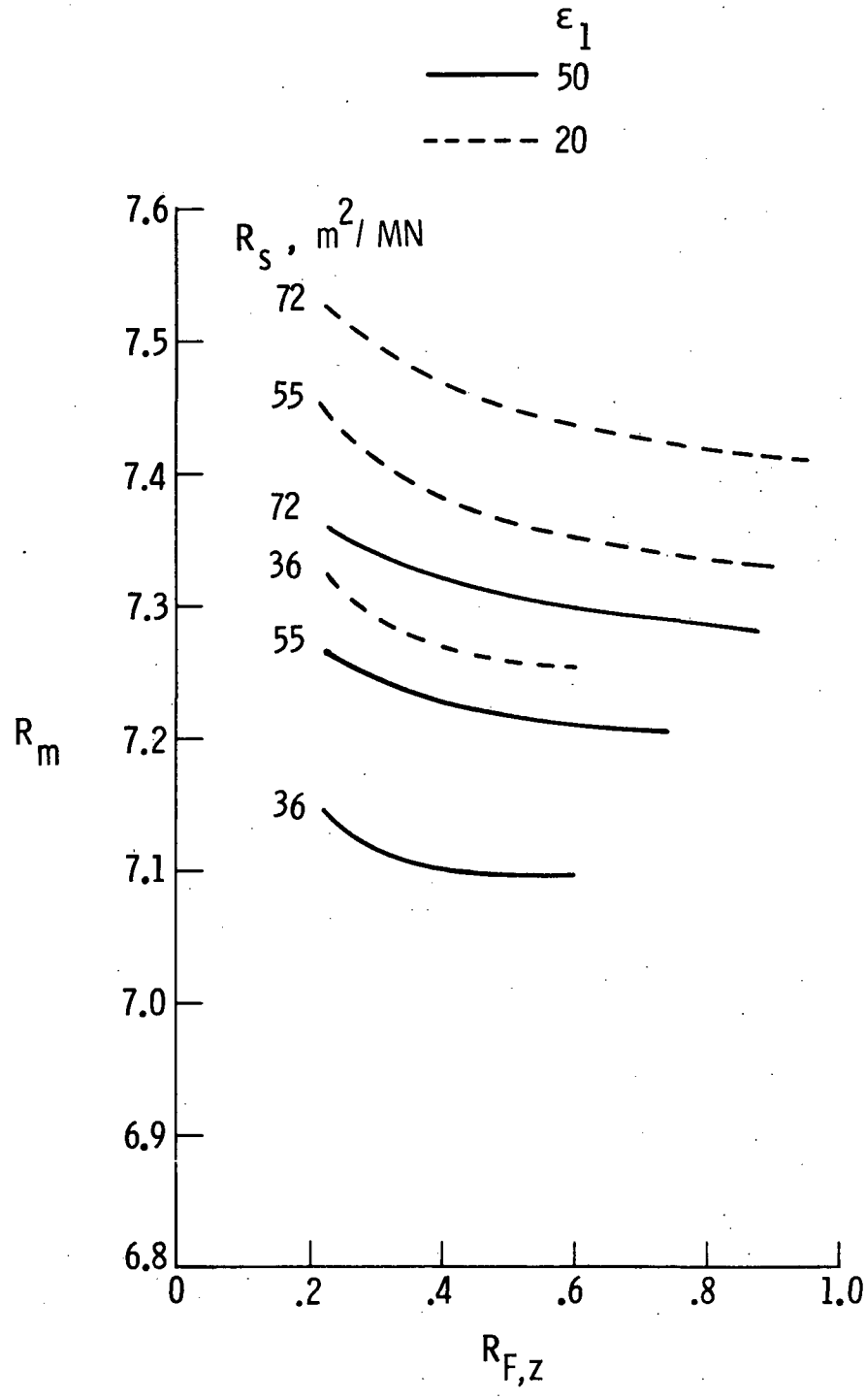

(c) Effect of ε_1.

Figure 9.- Continued.

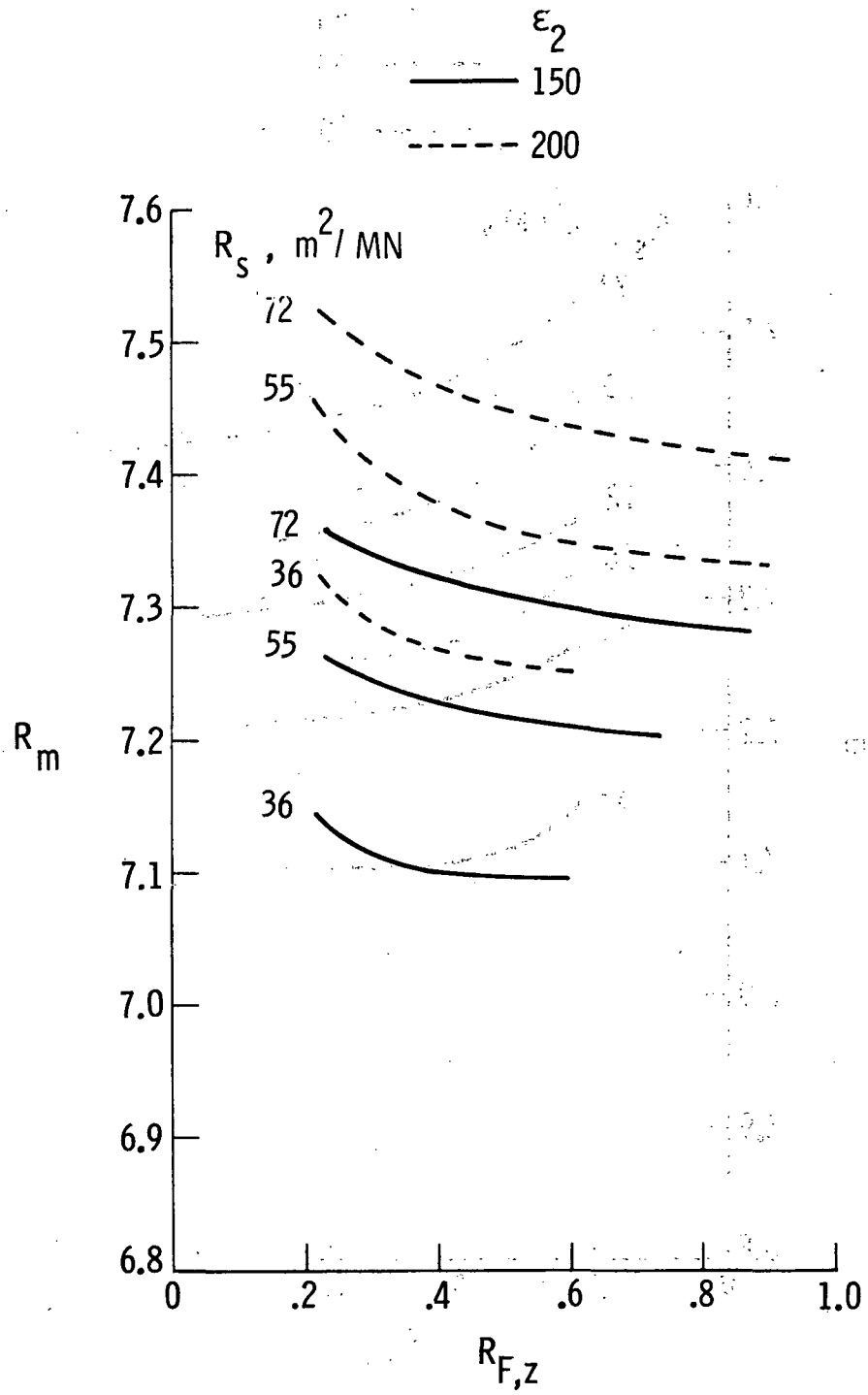

(d) Effect of ε_2.

Figure 9.- Concluded.

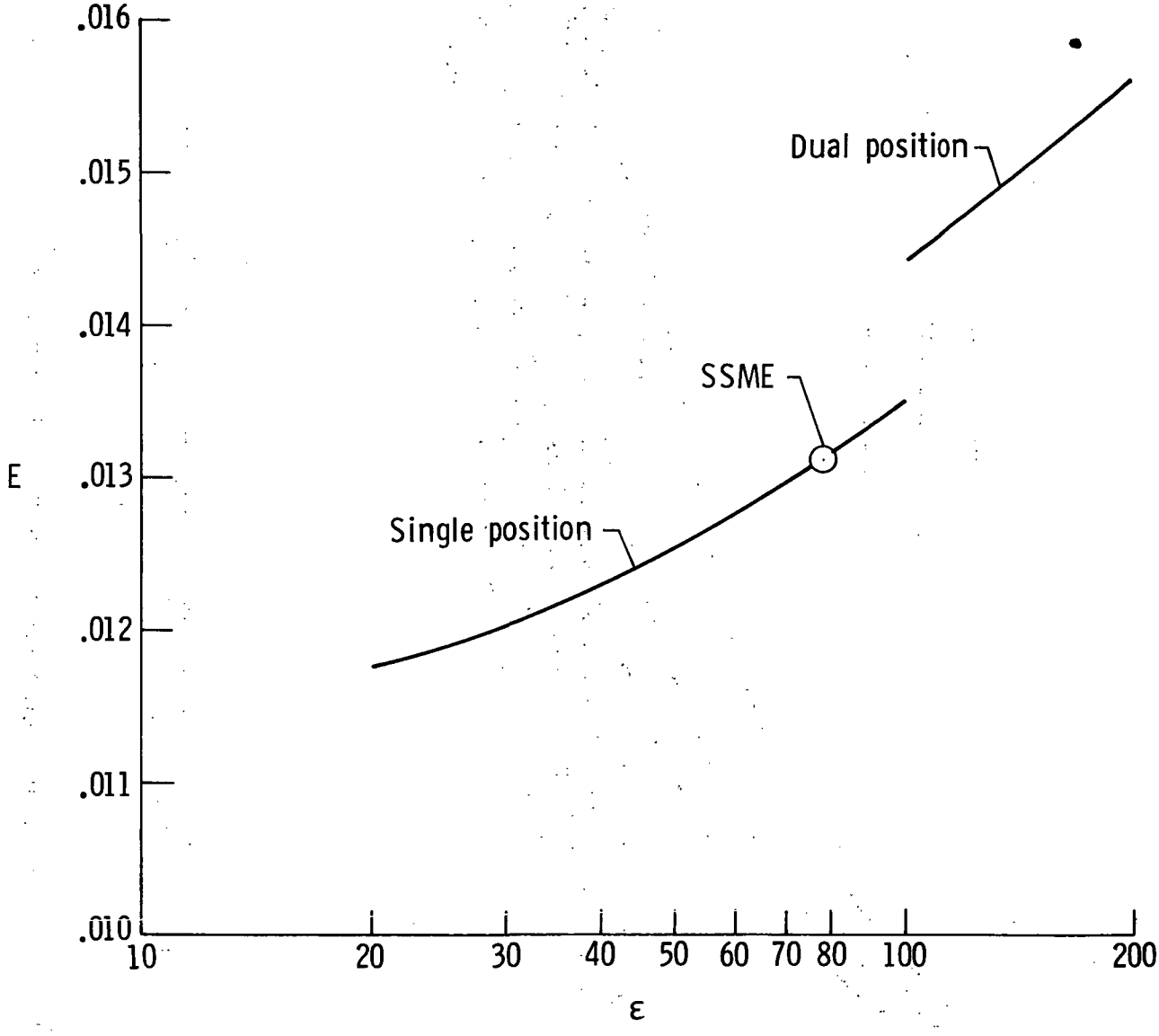

Figure 10.- Variation of engine mass coefficient with expansion ratio.

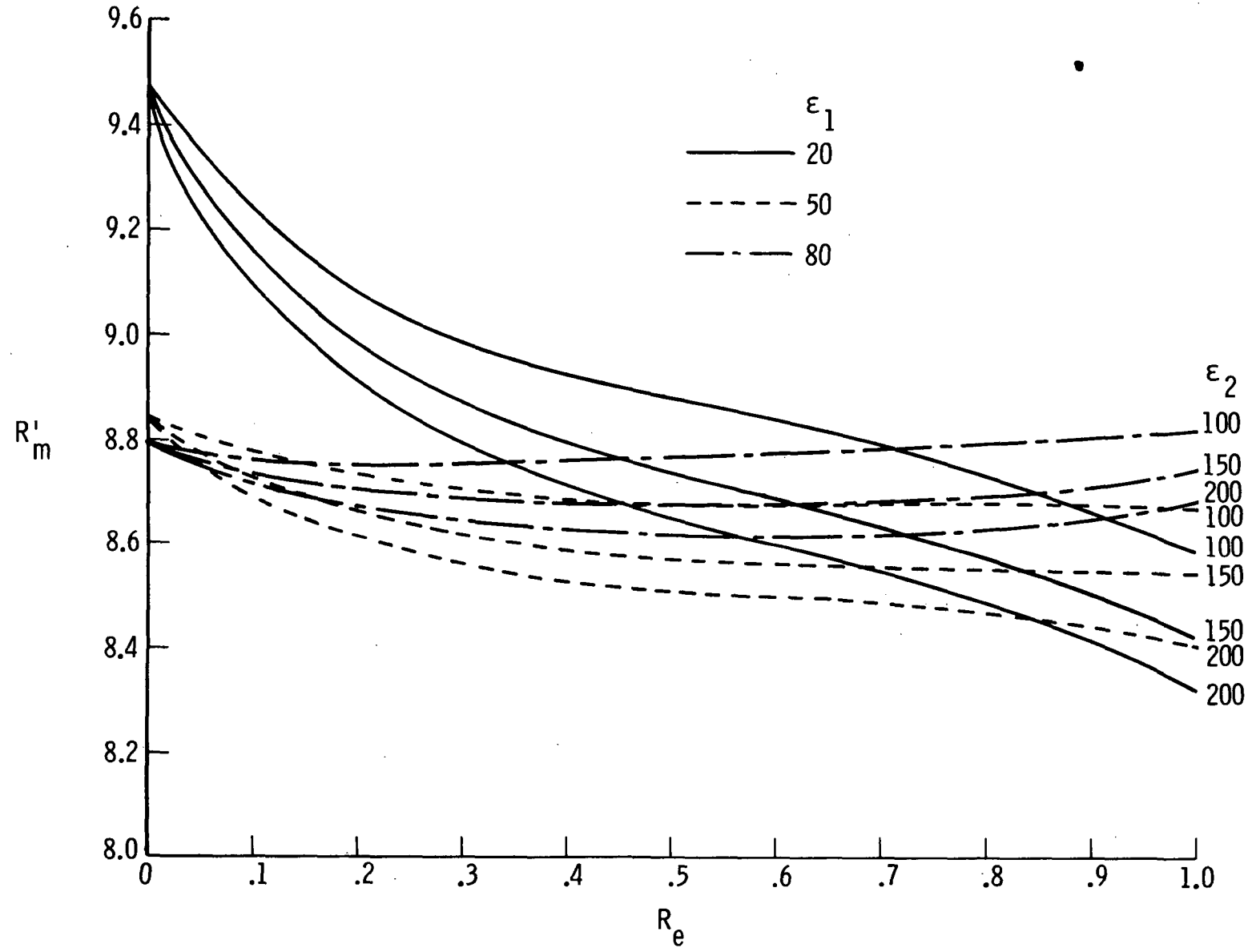

Figure 11.- Effect of engine mix ratio on vehicle sizing. $(T/W)_1 = 1.30$.

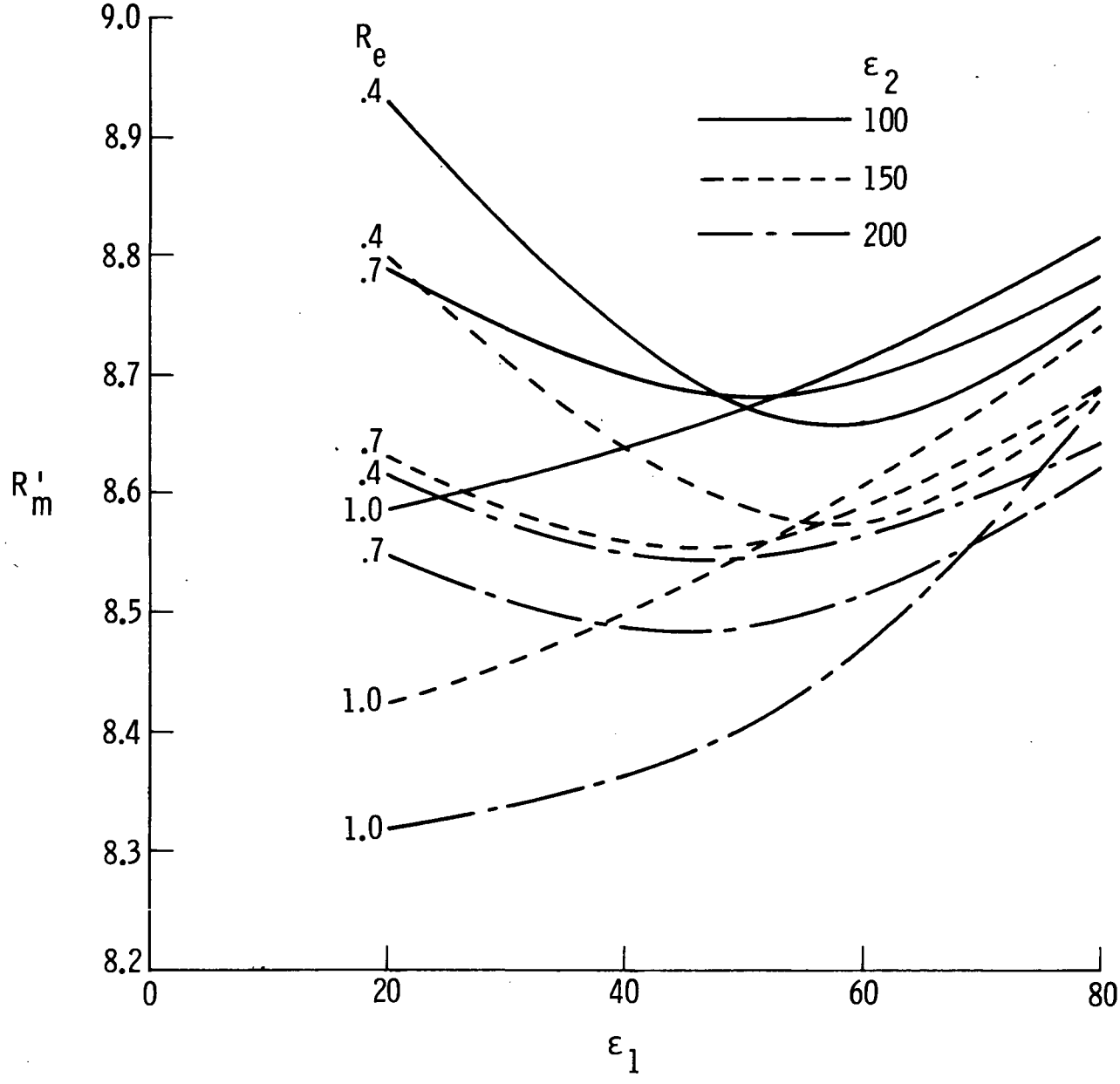

Figure 12.- Effect of initial expansion ratio on vehicle sizing. $(T/W)_1 = 1.30$.

1. Report No.	2. Government Accession No.	3. Recipient's Catalog No.
NASA TP-1045		

4. Title and Subtitle	5. Report Date
PARAMETRIC STUDY OF ASCENT PERFORMANCE OF A VERTICALLY LAUNCHED HYDROGEN-FUELED SINGLE-STAGE REUSABLE TRANSPORT	October 1977
	6. Performing Organization Code
7. Author(s)	8. Performing Organization Report No.
John J. Rehder	L-11533
	10. Work Unit No.
9. Performing Organization Name and Address	506-26-10-08
NASA Langley Research Center Hampton, VA 23665	11. Contract or Grant No.
	13. Type of Report and Period Covered
12. Sponsoring Agency Name and Address	Technical Paper
National Aeronautics and Space Administration Washington, DC 20546	14. Sponsoring Agency Code

15. Supplementary Notes

16. Abstract

The results of a parametric study of ascent performance characteristics are presented for a vertical-take-off, horizontal-landing, single-stage-to-orbit transport vehicle powered by hydrogen fuel rocket engines with a mixture of fixed- and dual-position nozzles. These data are intended to be used as a tool for rapidly providing accurate performance estimates as part of an integrated design procedure for advanced vehicles and as a guide for determining promising candidate configurations for more detailed study. The analysis has been made by systematically varying two sets of trajectory similarity parameters based on the propulsive and aerodynamic characteristics of the vehicle and by calculating a trajectory for each combination of the parameters. The propulsion parameters are the initial thrust-weight ratio, engine combination, and the two expansion ratios of the dual-position rocket nozzles. The aerodynamic parameters are the ratio of reference area to initial weight and the ratio of maximum allowable normal force to initial weight. The results from the propulsion parametric study were used in a first-order analysis to determine the effect on the performance of including the engine mass penalty. This analysis indicates that the configuration with the lowest initial mass for a given payload requires all dual-position nozzles with initial expansion ratio of 50 and a final expansion ratio of 150.

17. Key Words (Suggested by Author(s))

Ascent performance
Single-stage-to-orbit vehicle
Launch vehicle
Rocket propulsion

18. Distribution Statement

Unclassified - Unlimited

Subject Category 15

19. Security Classif. (of this report)	20. Security Classif. (of this page)	21. No. of Pages	22. Price*
Unclassified	Unclassified	39	$4.00

* For sale by the National Technical Information Service, Springfield, Virginia 22161

NASA-Langley, 1977

National Aeronautics and
Space Administration

Washington, D.C.
20546

Official Business
Penalty for Private Use, $300

THIRD-CLASS BULK RATE

Postage and Fees Paid
National Aeronautics and
Space Administration
NASA-451

NASA

POSTMASTER: If Undeliverable (Section 158
Postal Manual) Do Not Return